RESONANT AND NONRESONANT NONLINEAR OPTICAL SPECTROSCOPY OF CDSE QUANTUM DOTS FOR NONLINEAR PHOTONIC APPLICATIONS

JaeTae Seo*, SeongMin Ma, Qiguang Yang, Russell Battle, Linwood Creekmore, Ashley Jackson, Tifney Skyles, Patrice Scales, Kwang Lee, Devin Pugh-Thomas, and Bagher Tabibi
Department of Physics, Hampton University, Hampton, VA, 23668, U.S.A, * jaetae.seo@hamptonu.edu
William Yu and Vicki Colvin
Department of Chemistry, Rice University, Houston, Texas 77005, USA
SungSoo Jung
Korea Research Institute of Standards and Science, Daejeon, 305-600, South Korea

ABSTRACT

The cubic nonlinearity of semiconductor quantum dots with resonant (1h→2e) and nonresonant excitations was investigated with Z-scan and four-wave mixing (FWM) spectroscopy. Z-scan spectroscopy revealed positive nonlinear absorption and negative nonlinear refraction of CdSe quantum dots. The hyperpolarizability of the quantum dots with resonant degenerative FWM was almost two-orders higher than that with nonresonant excitation. The possible physical origins of the cubic nonlinearity of the quantum dots were dominant two-step resonant absorption with resonant excitation and multiple nonlinear processes including a large contribution of the electronic polarization process with both resonant and nonresonant excitations.

1. INTRODUCTION

Colloidal semiconductor nanocrystals have drawn significant attention because of their distinct roles in nonlinear photonic applications using large nonlinear optical properties with wide bandgap tunability. The nonlinear optical properties and applications of the colloidal semiconductor nanoscale materials significantly changes with resonant and nonresonant excitation processes. The processes leading to non-resonant nonlinearity are usually in relatively fast time scales, which are good candidates for optical switching and nonlinear transmission photonic applications. On the other hand, the processes causing resonant nonlinearity are usually in relatively slow time scales, which results in huge optical nonlinearity. Resonant nonlinear optical materials are widely utilized for Q-switching using a negative nonlinear absorption property, and for nonlinear transmission using a positive nonlinear absorption property as well as nonlinear refraction property or nonlinear phase changes.

In this paper, we present the resonant (1h→2e) and nonresonant nonlinear optical properties of CdSe nanocrystals using Z-scan and degenerate four-wave mixing (DFWM) by nanosecond laser pulse at 532 nm and 1064 nm (Continuum, Surelite II, Nd:YAG laser) with 6-ns pulse width and 10-Hz repetition rate.

2. EXPERIMENT

CdSe colloidal quantum-dot nanocrystals for Z-scan and DFWM spectroscopy were prepared by injecting Se solution (a mixture of Se, tributylphosphine (TOP), octadecene, and toluene) into the completely dissolved CdO (by stearic acid) solution (a mixture of octadecene, trioctylphosphineoxide (TOPO), and hexadecylamine) at 280 ^{o}C. Then, the CdSe colloidal quantum dots were collected at 240 ^{o}C in different time intervals to obtain CdSe nanocrystals with different sizes [1,2,3].

Numerous nonlinear optical spectroscopic techniques of wave mixing or transmission methods have been utilized to study nonlinear refraction and nonlinear absorption coefficients or third-order nonlinear susceptibility of optical materials [4,5,6,7,8,9]. For the transmission methods, the nonlinear refractive index coefficient (γ) of an optical material can be extracted from any closed Z-scan, closed I-scan and closed S-scan measurements [10], where Z is the sample position, I is the peak intensity of the input laser beam, $S(Z_a, r_a)$ is the linear transmittance at the aperture, Z_a is the displacement of the aperture from the focal plane, and r_a is the aperture radius size. I- and S-scan methods are useful when it is inconvenient to move the sample or when a sample's motion produces problems in Z-scan [10]. On the other hand, the nonlinear absorption coefficient (β) is obtained by using open Z-scan or open I-scan measurements. Z-scan and I-scan nonlinear spectroscopy have been used as a standard tool for measuring both nonlinear absorption and nonlinear refraction of optical materials. Both nonlinear spectroscopic techniques are simple and highly sensitive [4,11]. Closed Z-scan is based on self-focusing (valley-peak trace, positive nonlinearity) or defocusing (peak-valley trace, negative nonlinearity) of an optical beam through the nonlinear materials as shown in figure 1 (b) [12]. Using a single

Report Documentation Page

Form Approved
OMB No. 0704-0188

1. REPORT DATE	2. REPORT TYPE	3. DATES COVERED
01 NOV 2006	**N/A**	**-**

4. TITLE AND SUBTITLE	5a. CONTRACT NUMBER
Resonant And Nonresonant Nonlinear Optical Spectroscopy Of Cdse Quantum Dots For Nonlinear Photonic Applications	5b. GRANT NUMBER
	5c. PROGRAM ELEMENT NUMBER
6. AUTHOR(S)	5d. PROJECT NUMBER
	5e. TASK NUMBER
	5f. WORK UNIT NUMBER
7. PERFORMING ORGANIZATION NAME(S) AND ADDRESS(ES) **Department of Physics, Hampton University, Hampton, VA, 23668, U.S.A**	8. PERFORMING ORGANIZATION REPORT NUMBER
9. SPONSORING/MONITORING AGENCY NAME(S) AND ADDRESS(ES)	10. SPONSOR/MONITOR'S ACRONYM(S)
	11. SPONSOR/MONITOR'S REPORT NUMBER(S)

12. DISTRIBUTION/AVAILABILITY STATEMENT
Approved for public release, distribution unlimited

13. SUPPLEMENTARY NOTES
See also ADM002075., The original document contains color images.

14. ABSTRACT

15. SUBJECT TERMS

16. SECURITY CLASSIFICATION OF:			17. LIMITATION OF ABSTRACT	18. NUMBER OF PAGES	19a. NAME OF RESPONSIBLE PERSON
a. REPORT	b. ABSTRACT	c. THIS PAGE			
unclassified	**unclassified**	**unclassified**	**UU**	**49**	

Standard Form 298 (Rev. 8-98)
Prescribed by ANSI Std Z39-18

Gaussian laser beam, the transmittances of a nonlinear medium are related to the nonlinear susceptibilities.

The DFWM technique was also often utilized for measuring nonlinearity of optical materials through interaction between four light waves with the same angular frequency, in which three of the four light waves are the incident light and the another light wave is the signal or conjugate light.

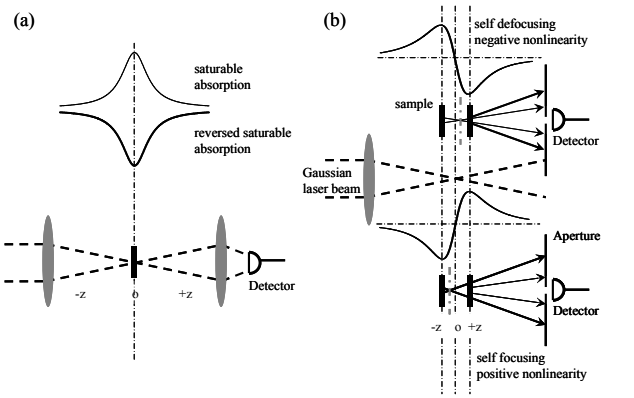

Fig. 1. Schematic diagram of open (a) and closed (b) Z-scan nonlinear spectroscopy.

In the forward DFWM experiment, two laser beams with wave vectors k_1 and k_2 were focused in coincidence on the sample, whose thickness was 1 mm, at a small angle of ~0.74°. The laser beam passed through an attenuator for intensity adjustment. The two spatially and temporally overlapped beams wrote a dynamic grating in the sample and then the beams themselves were diffracted by the grating in directions of $2k_1$-k_2 and $2k_2$-k_1, respectively. Since beam k_1 is much stronger than beam k_2, the signal in the $2k_1$-k_2 direction is much stronger than that in the $2k_2$-k_1. The diffracted signal in the $2k_1$-k_2 direction, which was proportional to the third-order nonlinear susceptibility $\chi^{(3)}$, was detected by a photomultiplier and boxcar average system.

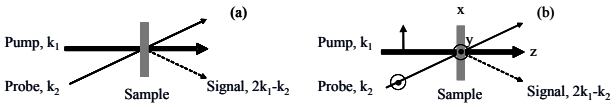

Fig. 2. Schematic diagrams of parallel (a) and orthogonal (b) DFWMs.

Polarization-dependent DWFM, as shown in figure 2, is a useful tool for measuring different components of $\chi^{(3)}_{ijkl}$ (where *ijkl=x, y, z*), of which allows the analysis of the contribution of electronic, molecular reorientation, and thermal contribution to the third-order nonlinearity. For orthogonal polarization between pump and probe waves, there are no intensity gratings, population gratings, and thermal gratings, because the intensity distribution of the interaction region is uniform. However, there will be an index grating due to the polarization modulation of the total field. The total electric fields of the incident light waves are [13]

$$E = \left(\hat{e}_x E_1 + \hat{e}_y E_2 e^{i\phi}\right) e^{-i\omega t}, \qquad (1)$$

where $\hat{e}_i$ is the unit direction vector (i=x, y), $E_1 = A_{pump} e^{ikz}$, $E_2 = A_{probe} e^{ik\,z\cos\theta}$, A_j is the amplitude of light waves (j= *pump, probe*), $\phi = \frac{2\pi}{\lambda} n_0 x \sin\theta$, λ is the wavelength of light, ω is the angular frequency of light, n_o is the linear refractive index of material, and θ is the interaction angle. The state of polarization of the total field is a periodic function of x. The various polarization states make a polarization grating in the material. The incident pump light wave is scattered by this polarization grating, which was formed by the pump and probe light waves.

3. OPTICAL PROPERTIES OF CDSE NANOCRYSTAL QUANTUM DOTS

The typical linear absorption spectra of colloidal CdSe quantum dots in toluene are shown in figure 3. The absorption spectra of semiconductor nanocrystals with size near the exciton Bohr radius clearly exhibit discrete features because of transitions coupling electron and hole quantized states. The semiconductor nanocrystals also exhibit a strong blue-shift of energy bandgap compared with that (~714 nm) of CdSe bulk materials because of their quantum confinement. The average diameter of CdSe nanocrystals was ~3.5 nm. Absorption peaks of CdSe nanocrystals were ~565, 537, 469 and 405 nm. Absorption coefficients ($\alpha = 2.3A/d$, $d = 1\ cm$) at 532 nm were 3.5, 1.5, 0.76, and 0.35 cm^{-1} for different concentrations in parallel DFWM, ~0.03, 0.09, 0.18, 0.25, and 0.34 cm^{-1} for different concentrations in orthogonal DFWM.

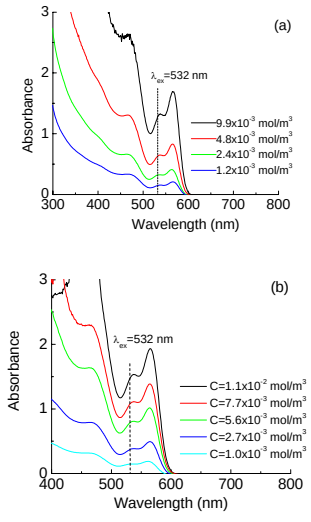

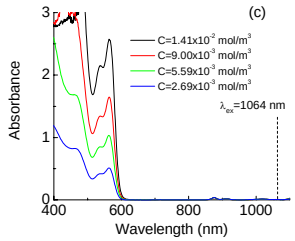

Fig. 3. Absorption spectra of CdSe nanocrystals in toluene for parallel (a) and orthogonal (b) resonant DFWMs and for parallel and orthogonal nonresonant DFWMs (c). Average diameter of CdSe nanocrystals was ~3.5 nm, Exciton absorption peaks were ~565 (1h→1e), 537 (1h→2e), 469 (1h→3e), and 405 nm (1h→4e).

The linear refractive index of CdSe nanocrystals was calculated to be ~2.34 for ~3.5 nm average diameter [14],

$$n_{CdSe} = \sqrt{1 + \frac{(\varepsilon_{bulk} - 1)}{1 + \left(\frac{0.75}{D}\right)^{1.2}}}, \qquad (2)$$

where, ε_{bulk} ~ 6.2 is the dielectric constant of bulk CdSe, and D is the average diameter of CdSe quantum dots in nm unit.

The third-order nonlinear coefficients of CdSe quantum dots were estimated by measuring the transmittance of a nonlinear medium through a finite aperture in the far field as a function of the sample position Z with respect to the focal plane. The open and closed Z-scans were used to estimate the nonlinear absorption and refraction coefficients, respectively. The laser power transmission through the sample was measured with open and closed apertures in the far-field region as a function of the position of the sample [15, 16],

$$T(z, S=1) = \sum_{m=0}^{\infty} \frac{\left(\frac{-q}{1+z^2/z_0^2}\right)^m}{(m+1)^{3/2}}, \text{ for } q<1 \qquad (3)$$

The normalized transmittance of a nonlinear medium for the open aperture ($S=1$) Z-scan and I-scan spectroscopy is a function of nonlinear absorption (β), where $q(r,z,t) = \beta I(r,z,t) L_{eff}$, $L_{eff} = (1-e^{-\alpha L})/\alpha$, L=1 mm is the thickness of the sample, α is the linear absorption coefficient and β is the nonlinear absorption coefficient. The condition of the thin sample approximation, $z_0 = \pi\omega_0^2/\lambda$ ~ 1.2 mm > L, was satisfied, where z_0 is the Rayleigh range, ω_0 is the beam radius at the focal plane and λ is the laser wavelength. The linear transmittance of the aperture for a spatial Gaussian input beam is $S = 1 - exp\left(-2r_a^2/w_a^2\right)$, where r_a is the aperture radius, and ω_a is the beam radius at the aperture in the linear regime. Sensitivity of the difference between the normalized peak and valley transmittance increases for smaller linear transmittance of the aperture (S<<1) for the given phase shift . The on-axis normalized transmittance through a nonlinear absorptive and refractive material for the closed aperture (S<<1) and I-scan spectroscopy is given by [17],

$$T_{ra}(z, S<<1) = 1 - \frac{4\Delta\Phi_0 x + q(3+x^2)}{(1+x^2)(9+x^2)} - \frac{4\Delta\Phi_0^2(5-3x^2) - 8\Delta\Phi_0 qx(9+x^2) - q^2(40+17x^2+x^4)}{(1+x^2)(9+x^2)(25+x^2)} \qquad (4)$$

where $x = -\left(\frac{1}{z_0}\right)\left(z + \frac{z_0^2 + z^2}{d_{sa} - z}\right)$ or $x = -\frac{z}{z_0}$ for $d >> z_0$, is the linear phase parameter, d_{sa} is the propagation distance from the sample to the aperture plane, $\Delta\Phi_o(t) = k\gamma I_o(t) L_{eff}$ is the on-axis phase shift, I_0 is the laser intensity at the focus, and γ is the nonlinear refraction coefficient.

The nonlinear refraction and absorption coefficients of the sample (dots in matrix) are assumed to be an addition of that of quantum dot and matrix contributions [18]. The total third-order nonlinear susceptibility of the dilute solution (volume fraction << 1) is given by [19, 20],

$$\chi_{tot}^{(3)} = \chi_{dot\_eff}^{(3)} + \chi_{toluene}^{(3)}, \qquad (5)$$

where, $\chi_{tot}^{(3)}$ and $\chi_{toluene}^{(3)}$ are the third-order nonlinear susceptibilities of the sample (dots in matrix) and toluene, and $\chi_{dot\_eff}^{(3)}$ is the effective third-order nonlinear susceptibility of CdSe quantum dots. The effective third-order nonlinear susceptibility $\chi_{dot\_eff}^{(3)}$ includes the dielectric effect of nanocrystals and toluene. Therefore, the effective third-order nonlinear susceptibility of quantum dots is given by simply subtracting the third-order susceptibility of toluene from the $\chi_{tot}^{(3)}$ of the sample (dots in matrix). The nonlinear transmittance of closed and open Z-scan of pure CdSe semiconductor nanocrystals (figure 6) were extracted by simply dividing that of CdSe dots in toluene (figure 4) with that of toluene (figure 5) for a same input intensity. The sign of nonlinearities of CdSe quantum dots and toluene matrices were negative nonlinearities (self-defocusing) and positive (self-focusing), respectively. The nonlinear refraction and absorption coefficients of pure

toluene were extrapolated by fitting with the nonlinear transmittance using the equations (3) and (4). The third order nonlinear susceptibility of pure CdSe was estimated with the following equation using the nonlinear refraction and absorption coefficients,

$$\chi^{(3)} = \sqrt{\left(Re\chi^{(3)}\right)^2 + \left(Im\chi^{(3)}\right)^2}\,, \qquad (6)$$

where, $Re\chi^{(3)} = \frac{4}{3} n_o^2 \varepsilon_o c\gamma$ is the real part of $\chi^{(3)}$, and $Im\chi^{(3)} = \frac{1}{3\pi} n_o^2 \varepsilon_o c\lambda\beta$ is the imaginary part of $\chi^{(3)}$.

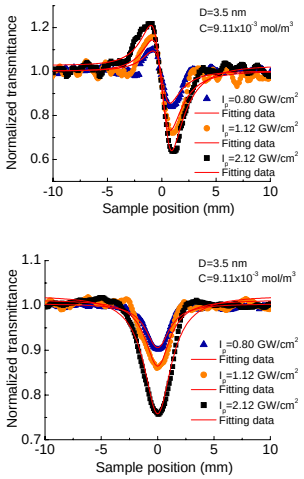

Fig. 4. Nonlinear transmittance of closed and open Z-scan of CdSe NCs in toluene. The nonlinear refraction and absorption coefficients of CdSe NCs in toluene were -1.94×10^{-17} m^2/W and 6.50×10^{-11} m/W at 532-nm wavelength and in 6-ns pulse width. The diameter and concentration of NCs were 3.5 nm and 9.11×10^{-3} mol/m^3.

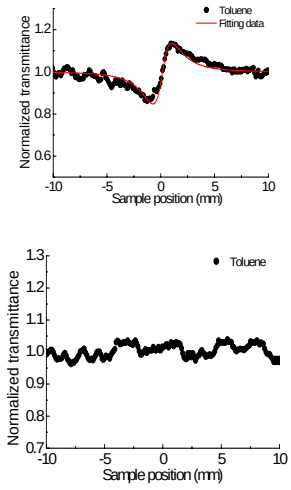

Fig. 5. Nonlinear transmittance of closed and open Z-scan of toluene. The nonlinear refraction coefficient of CdSe NCs in toluene was 4.85×10^{-18} m^2/W at 532-nm wavelength and in 6- ns pulse width.

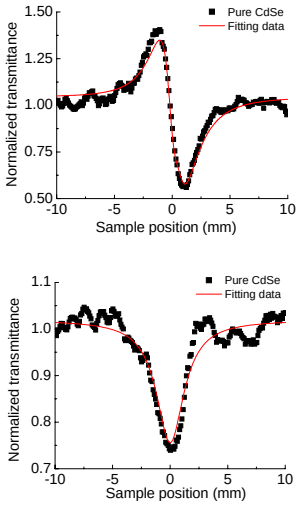

Figure 6. Nonlinear transmittance of closed and open Z-scan of pure CdSe NCs. The nonlinear refraction and absorption coefficients of CdSe NCs in toluene were -9.55×10^{-18} m^2/W and 4.49×10^{-11} m/W at 532-nm wavelength and in 6-ns pulse width. The diameter and concentration of NCs were 3.5 nm and 9.11×10^{-3} mol/m^3. The positive nonlinear absorption with resonance excitation implies that the absorption cross-section of the excited state is larger than that of the ground state.

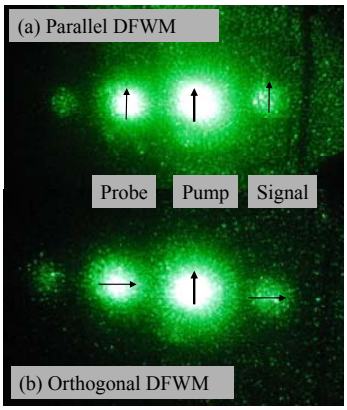

Fig. 7. The pictures show the probe, pump, and self-diffraction light from the CdSe quantum dot sample for parallel (a) and orthogonal (b) DFWMs.

In the polarization dependent DFWM experiment, the angle of interaction or diffraction and the Kein and Cook parameter Q were ~0.74° and 2.96, respectively. The Kein-Cook parameter is given as $Q \equiv 2\pi L_g \lambda / n_0 \Lambda^2$, where, L_g is the grating thickness, and Λ is the grating pitch [21]. The diffraction from the laser induced gratings with small Q (i.e., Q≤1) is called Raman-Nath diffraction. However, the scattering light from the grating with large Q≥10 is called Bragg diffraction. Figure 7 shows the probe, pump, and self-diffracted light. The first light is the diffraction light of the

probe light from the laser induced gratings, and the second and third light are the probe, and pump light, respectively. The fourth light is the self-diffracted light or signal beam of the pump from the laser induced gratings. The clear multiple diffractions imply that the Raman-Nath diffraction effect is still dominant for the Kein and Cook parameter Q ~ 2.96.

Figure 8 shows logarithmic plots of the DFWM signal from CdSe nanocrystals with resonance (1h→2e, a and b) and nonresonant (c and d) excitations as a function of total pump intensity at around zero delay. The input pump irradiance level was increased from ~1 MW/cm^2 to ~100 MW/cm^2 during the measurement of the signal intensity via the pump intensity near zero delay. The signal intensity was varied as $I^{2.9\sim3.1}$ for parallel DFWM and $I^{2.70\sim3.16}$ for orthogonal DFWM with resonant excitation indicating the dominance of a third order nonlinearity. Also, the FWM signal intensity had a strong cubic dependence of $I^{3.0\sim3.05}$ for parallel DFWM and an $I^{2.99\sim3.09}$ for orthogonal DFWM to the nonresonant excitation intensity at 1064 nm, which indicated a cubic nonlinearity. Thus the third-order nonlinearity of the samples can be safely extracted from the degenerate four-wave mixing measurement in this intensity range.

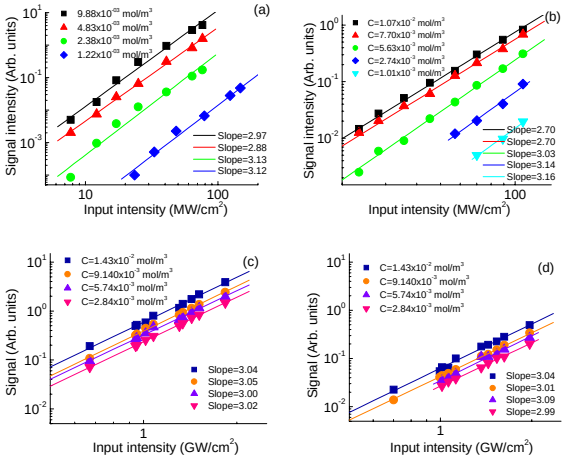

Fig. 8. Logarithmic plot of the parallel and orthogonal DFWM signals (a, b) in CdSe nanocrystals at 532 nm and those (c, d) at 1064 nm as a function of total pump intensity at around zero delay.

The third-order nonlinear susceptibilities of samples (CdSe dots in toluene or toluene itself) were estimated using the following equation (7) for resonant excitation at 532 nm and equation (8) for nonresonant excitation at 1064 nm by comparison of the FWM signal beams of samples with that of CS_2 measured under identical conditions [22],

$$\chi_S^{(3)} = \sqrt{\frac{I_S}{I_R}}\left(\frac{n_S}{n_R}\right)^2\left(\frac{L_R}{L_S}\right)\left(\frac{\alpha L}{e^{-\alpha L/2}\left(1-e^{-\alpha L}\right)}\right)\chi_R^{(3)} \qquad (7)$$

$$\chi_S^{(3)} = \sqrt{\frac{I_S}{I_R}}\left(\frac{n_S}{n_R}\right)^2\left(\frac{L_R}{L_S}\right)\chi_R^{(3)} \qquad (8)$$

where I is the intensity of the FWM signal beam, n is the linear refractive index ($n_s(CdSe)$: given by equation (2), $n_R(CS_2)\sim1.63$ [23]), L ($L_s=L_R=1$ *mm*) is the sample path length in DFWM, $\alpha = 2.3A/d$, $d = 1$ *cm* , see figure 1) is the linear absorption coefficient of the sample at 532 nm, and S and R indicate sample and reference. The excellent and stable third-order optical response solvent, carbon disulfide (CS_2, 99+ %, spectrophotometric grade, Aldrich), was selected as a reference. It has been assumed that the reference has no linear absorption at the excitation wavelength at both 532 and 1064 nm. The absorption length of CdSe in toluene for resonant DFWM experiment was L ~ 0.35, 0.15, 0.076, and 0.035 << 1 in parallel DFWM and ~0.03, 0.09, 0.18, 0.25, and 0.34 in orthogonal DFWM for each of the different concentrations as listed in the figure 3 (a) and (b). Therefore, the equation (7) is appropriate to calculate the third-order nonlinearity for the Kerr-like medium.

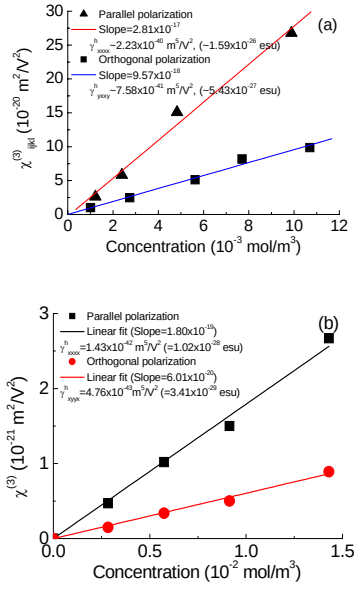

Fig. 9. Resonant (1h→2e, a) and nonresonant (b) third-order nonlinear susceptibility as a function of concentration of CdSe nanocrystals. The slope of linear fitting revealed the hyperpolarizability of CdSe nanocrystals.

The effective third-order macroscopic susceptibility of the sample (dots in matrix) is assumed to be an addition of that of quantum dot and matrix contributions [18,19,20]. The third-order nonlinear susceptibilities of pure CdSe semiconductor nanocrystals were simply subtracted from that of CdSe dots in toluene with that of toluene. The third-order susceptibilities $\chi^{(3)}_{xxxx}$ and $\chi^{(3)}_{yxxy}$ of pure toluene were measured to be ~1.58×10^{-21} m^2/V^2 (1.13×10^{-13} esu) and ~1.13×10^{-21} m^2/V^2 (8.07×10^{-14} esu) respectively, comparing

with the reference sample CS_2. The ratio of third order nonlinearities $\chi^{(3)}_{yxxy}/\chi^{(3)}_{xxxx}$ of toluene was 0.72, which indicated a large contribution of molecular reorientation process to the third-order nonlinearity of toluene [24]. The third order nonlinear susceptibility $\chi^{(3)}_{xxxx}$ and the linear refractive index of CS_2 were reported to be ~9.5×10^{-21} m^2/V^2 (~6.8×10^{-13} esu) and ~1.63 at 532 nm in the nanosecond time-scale [25]. Therefore, the effective third-order nonlinear susceptibilities $\chi^{(3)}_{xxxx}$ and $\chi^{(3)}_{yxxy}$ of semiconductor nanocrystals were ~7.9×10^{-21} – 2.5×10^{-19} m^2/V^2 (~5.7×10^{-13} – 1.8×10^{-11} esu) for various concentrations of quantum dots 1.2×10^{-6} – 9.9×10^{-6} mol/L in toluene and ~1.02×10^{-20} – 9.86×10^{-20} m^2/V^2 (~7.31×10^{-13} – 7.06×10^{-12} esu) for various concentrations of quantum dots ~1.01×10^{-3} – 1.07×10^{-2} mol/m^3 in toluene.

The third-order nonlinear susceptibility of the CdSe nanocrystals is correlated with the dot concentration and the effect of the dielectric confinement [26],

$$\chi^{(3)} = f^4 N_a \gamma^h C \quad (SI), \tag{9}$$

where $f = \dfrac{3n_{toluene}^2}{n_{dot}^2 + 2n_{toluene}^2}$ is the local field factor, n is the refractive index ($n_{dot}=n_s$: given by equation (1), $n_{toluene}$~*1.5* [22]), N_a is Avogadro's number, and C is the concentration of CdSe quantum dots. The second-order hyperpolarizability (γ^h) of CdSe nanocrystals was extrapolated from the slope $(f^4 N_a \gamma^h)$ of the third-order nonlinear susceptibility as a function of concentration plot as shown in figure 9. The resonant and nonresonant hyperpolarizabilities γ^h_{xxxx} and γ^h_{yxxy} and of CdSe nanocrystals with parallel and orthogonal DFWMs were estimated to be ~2.23×10^{-40} m^5/V^2 (~1.58×10^{-26} esu), ~7.58×10^{-41} m^5/V^2 (~5.43×10^{-27} esu), ~1.43×10^{-42} m^5/V^2 (~1.02×10^{-28} esu), and ~4.76×10^{-43} m^5/V^2 (~3.41×10^{-29} esu) respectively. The hyperpolarizability ratios $\gamma^h_{yxxy}/\gamma^h_{xxxx}$ of resonant and nonresonant were ~0.34 which indicated a large contribution of electronic polarization process to the third-order nonlinearity of CdSe quantum dots. The unit conversion between $\chi^{(3)}$ and γ^h was made based on the following relationships [27],

$$\chi^{(3)}\left[\frac{m^2}{V^2}, SI\right] = \frac{4\pi\times10^{-8}}{9}\chi^{(3)}[esu],$$

and

$$\gamma^h\left[\frac{m^5}{V^2}, SI\right] = \frac{4\pi\times10^{-14}}{9}\gamma^h[esu]. \tag{10}$$

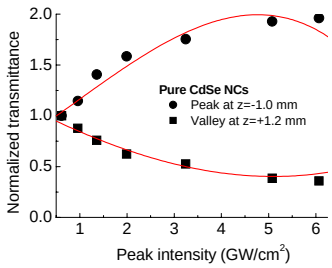

Figure 10. Nonlinear transmittance property (lower trace) at Z~1.2 mm (valley position) and saturable behaviour (upper trace) at z~ -1.0 mm (peak position) of CdSe quantum dots as a function of laser input intensity with resonant excitation. The diameter and concentration of NCs were 3.5 nm and 9.11×10^{-3} mol/m^3. The nonlinear transmittance threshold of CdSe quantum dots was ~3.3 GW/cm^2.

For the nonlinear transmittance photonic application, the total absorption is associated with linear and nonlinear absorptions ($\alpha=\alpha_o+\beta I$), and the total refraction is related with linear and nonlinear refraction ($n=n_o+\gamma I$). As the incoming laser intensity increases, the total absorption and refraction of the optical material is increased. Even the weak incoming laser can be reduced or totally blocked by the large nonlinearity of the optical materials. Also, the location of the nonlinear medium is critical to the operation of the refractive nonlinear photonic device. A self-focusing nonlinear photonic device works best if the nonlinear optical medium is placed approximately at a valley or at a Rayleigh range before the intermediate focus of the device. Positive nonlinear optical materials reduce the effective focal length of the focusing lens, and the laser beam in device is diffracted further at the exit aperture. Hence, the nonlinear transmittance is effectively reduced or blocked. For self-defocusing materials, the optimum position of materials in the nonlinear photonic device is approximately a Rayleigh range after the focus. Negative nonlinear optical materials diffract further the laser beam after focusing, because of the self-defocusing. Therefore, the self-focusing or the self-defocusing effect in the system results in effective reduction of nonlinear optical transmission.

The normalized transmission after the pinhole was measured as a function of input power intensity as shown in Figure 10 for the nonlinear transmittance experiment. The sample of CdSe quantum dots in toluene was placed at z ~ 1.2 mm at the near valley of the closed Z-scan (figure 6 (a) transmittance). The normalized transmittance after the pinhole depended on several parameters such as intensity, nonlinear absorption, nonlinear refraction, position of sample, Rayleigh range, effective length of sample, and distance between the sample and the aperture as shown in equation (4). Typical nonlinear transmittance behaviour of CdSe nanocrystals in toluene was shown in figure 10. The nonlinear transmittance threshold, which was a half of linear transmittance, of the

CdSe quantum dots was ~3.3 GW/cm^2. The laser power after pinhole was effectively reduced or blocked, when the sample CdSe quantum dots was placed around the valley area of the Z-scan measurement, because of an increase in total absorption and total refraction as well as a large phase change with increasing the input intensity.

4. CONCLUSIONS

In conclusion, CdSe quantum dots with average size at the near Bohr radius were synthesized using a colloidal chemical reaction. The CdSe nanocrystals exhibited strong blue shift and discrete energy states which were significantly modified from bulk crystals. Z-scan spectroscopy revealed that positive nonlinear absorption and negative nonlinear refraction of CdSe quantum dots. The hyperpolarizability of CdSe colloidal quantum dots with resonant excitation was almost two-order bigger than that with nonresonant excitation. Therefore, the positive nonlinear absorption with resonant excitation implies the existence of an electronic two-step absorption process and the larger absorption cross-section of excited state than that of ground state. It is well known that resonant excitation enhances the third-order nonlinearity significantly since many processes, such as electronic processes of two-step absorption or electronic polarization effect, nuclear processes, and even thermal processes, may contribute to the optical nonlinearity significantly. The possible thermal effect under long pulse laser irradiation is a disadvantage for the photonic device applications. The hyperpolarizability ratio $\gamma^h_{yxxy}/\gamma^h_{xxxx}$ of pure CdSe nanocrystals with either resonant or nonresonant excitations was ~0.34 which indicated a large contribution of the electronic polarization process to the cubic nonlinearity of CdSe quantum dots. The reduction threshold, which was a half of the linear transmittance, of CdSe quantum dots was ~3.3 GW/cm^2.

ACKNOWLEDGEMENTS

This work at Hampton University was supported by Army Research Laboratory (DAAD17-02-C-0107), Army Research Office (W911NF-04-1-0393), and National Science Foundation (EEC-0532472, HRD-0400041, PHY0139048).

REFERENCES

[1] Yu, W. W., Peng, X., 2002: Formation of High-Quality CdS and Other II-VI Semiconductor Nanocrystals in Noncoordinating Solvents:T unable Reactivity of Monomers, *Angew. Chem. Int. Ed.* **41**, 2368-2371.

[2] Yu, W. W., Wang, Y. A., Peng, X., 2003: Formation and stability of size-, shape-, and structure-controlled CdTe nanocrystals: ligand effects on monomers and nanocrystals, *Chem. Mater.* **15**, 4300-4308.

[3] Yu, W. W., Falkner, J. C., Shih, B. S., Colvin, V. L., 2004: Preparation and characterization of monodisperse PbSe nanocrystals in a non-coordinating solvent, *Chem. Mater.* **16**, 3318-3322.

[4] Sheik-Bahae M., Said A. A., Wei T., Hagan D. J., and Stryland E. W. V., 1990: Sensitive Measurement of Optical Nonlinearities Using a Single Beam, *IEEE J. Quantum Electron.*, **26**, 760-769.

[5] Friberg S. R, and Smith P. W., 1987: Nonlinear Optical Glasses for Ultrafast Optical Switches*, IEEE J. Quantum Electron.* **QE-23**, 2089-2094.

[6] Adair R., Chase L. L., and Payne S. A., 1987: Nonlinear refractive-index measurements of glasses using three-wave frequency mixing, *J. Opt. Soc. Am. B* **4**, 875-881.

[7] Moran M. J., She C. Y., and Carman R. L., 1975: Interferometric Measurements of the Nonlinear Refractive-Index Coefficient Relative to CS2 in Laser-System-Related Materials, *IEEE J. Quantum Electron,* **QE-11**, 259-263.

[8] Owyoung A., 1973: Ellipse Rotation Studies in Laser Host Materials, *IEEE J. Quantum Electron.* **QE-9**, 1064-1069.

[9] Hamad A. Y., Wicksted J. P., Wang S. Y., and Cantwell G., 1995: Spatial and temporal beam reshaping effects using bulk CdTe, *J. Appl. Phys.* **78(5)**, 2932-2939.

[10] Yang Q., Seo J. T., Creekmore S. J., Temple D., Yoo K. P., Kim S. Y., Jung S. S., and Mott A., 2003: Distortions in Z-scan Spectroscopy, *Appl. Phys. Lett.,* **82(1)**, 19-21.

[11] Chapple P. B., Staromlynska J., Hermann J. A., McKay T. J., and McDuff R. G., 1997: Single-Beam Z-Scan: Measurement Techniques and Analysis, *J. of Nonlinear Optical Physics and Materials*, **6(3)**, 251-293.

[12] Hashimoto T., Yamamoto T., Kato T., and Nasu H., 2001: *Z*-scan analyses for PbO-containing glass with large optical nonlinearity, *J. of Appl. Phys*. **90(2)**, 533-537.

[13] Slussarenko S., Francescangeli O., Simoni F., and Reznikov Y., 1997: High resolution polarization gratings in liquid crystals, *Appl. Phys. Lett.* **71**. 3613-3615.

[14] Wang L. W. and Zunger A., 1996: Pseudopotential calculations of nanoscale CdSe quantum dots, *Phys. Rev. B*. **53**, 9579-9582.

[15] Seo J. T., Ma S., Lee K., Tabibi B., Rankins C., Muhoro P., Mangana J., Pompey C., Creekmore S., Xie Z., Peng X., Qu J., Yu W., Wang A., Jung S., and Ruh H., 2004: Cadmium chalcogenide semiconductor nanocrystals for optical power limiting application, *Phys. Stat. Sol. (c)* **1**, 771-774.

[16] Seo J. T., S. Ma M., Lee K., Brown H., Jackson A., Skyles T., Cubbage N. M., Tabibi B., Yoo K. P., kim S. Y., Jung S. S., and Namkung M., 2005: highly porous

silica nanoaerogel for ultrafast nonlinear optical application, *Key Engineering Materials,* **287**, 352-356.

[17] Seo J. T., Yang Q., Creekmore S., Temple D., Yoo K. P., Kim S. Y., Mott A., Namkung M., and Jung S. S., 2003: Large and pure refractive nonlinearity of nanostructure silica aerogel, *Appl. Phys. Lett.*, **82(25)**, 4444-4446.

[18] Sun W., Patton T., Stultz L., andClaude J. P., 2003: Resonant third-order nonlinearities of tetrakis diruthenium complexes, *Opt. Comm.* **218**, 189-194.

[19] Sipe J. E. and Boyd R. W., 1992: Nonlinear susceptibility of composite optical materials in the Maxwell Garnett model, *Phy. Rev. A,* **46(3)**, 1614-1629.

[20] Zyss J., Chemla D. S., 1987: *Nonlinear Properties of Organic Molecules and Cystals*, Academic, Orlando.

[21] Petris A., Damzen M. J., and Vlad V. I., 2000: Enhanced wave mixing in photorefractive rhodium-doped barium titanate crystals, *Opt. Comm.* **176**, 223-229.

[22] Sutherland R. L., 1996: *Handbook of Nonlinear Optics,* Marcel Dekker, Inc., 390 pp., 457-458 pp.

[23] Illine B., Evain K., and Guennec M. L., 2003: A way to compare experimental and SCRF electronic static dipole polarizability of pure liquids, *J. Mol. Struct. (Theochem)* **630**, 1-9.

[24] Nalwa H. S., 1997: *Nonlinear optics of organic molecules and polymers*, edited by Nalwa H. S. and Miyata S., CRC Press, Inc., 571 pp.

[25] Wang P., Ming H., Xie J., Zhang W., Gao X., Xu Z., and Wei X., 2001: Substituents effect on the nonlinear optical properties of C60 derivatives, *Opt. Comm.* **192**, 387-391.

[26] Yu B., Zhu C., and Gan F., 1997: Optical Nonlinearity of Bi2O3 nanoparticles studied by Z-scan technique, *J. Appl. Phys.* **82(9)**, 4532-4537.

[27] Zhan X., Liu Y., Zhu D., Liu X., Xu G., and Ye P., 2001: Large third-order nonlinear optical response of a conjugated copolymer consisting of 2,5-diethylthiophene and carbzole units, *Chem. Phys. Lett.* **343**, 493-498.

Resonant and Nonresonant Nonlinear Optical Spectroscopy of CdSe Quantum Dots for Nonlinear Photonic Application

J. T. Seo, S. M. Ma, Q. Yang, R. Battle, L. Creekmore, A. Jackson, T. Skyles, P. Scales, K. Lee, D. Pugh-Thomas, and B. Tabibi

Department of Physics, Hampton University, Hampton, VA, 23668, U.S.A.

W. Yu and V. Colvin

Department of Chemistry, Rice University, Houston, Texas 77005, U.S.A

S. S. Jung

Korea Research Institute of Standards and Science, Daejeon, 305-600, South Korea

This work at Hampton University was supported by Army Research Laboratory (DAAD17-02-C-0107), Army Research Office (W911NF-04-1-0393), and National Science Foundation (HRD-0630372, HRD-0400041, NSF-PHY0139048)

Goals and Applications

- Goals
  - Development of CdSe nanoscale materials with large optical nonlinearity and high nonlinear figure of merit
  - Utilization of the nanoscale materials for nonlinear photonic applications

- Applications
  - *Nonlinear Transmittance Device*
    - Homeland security and battlefield enhancement
    - Optical pulse power shaping
  - All-optical switching
    - Ultrafast nonlinear response time
  - Passive Q-Switching
    - Saturable absorption
  - Biomedical Applications

Experiment Setup
for Semiconductor Nanocrystal Synthesis

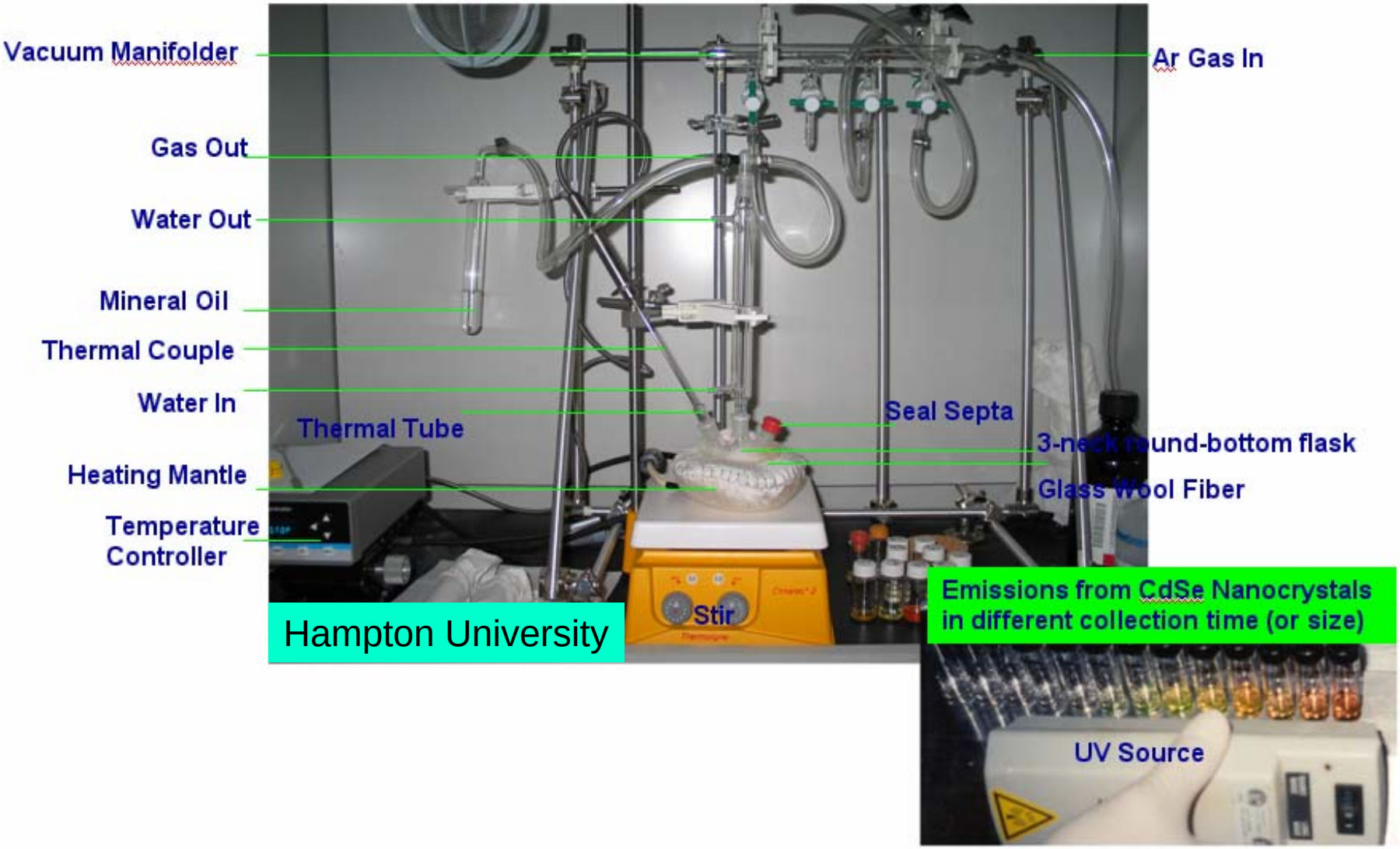

Semiconductor Bulk and Nanocrystals

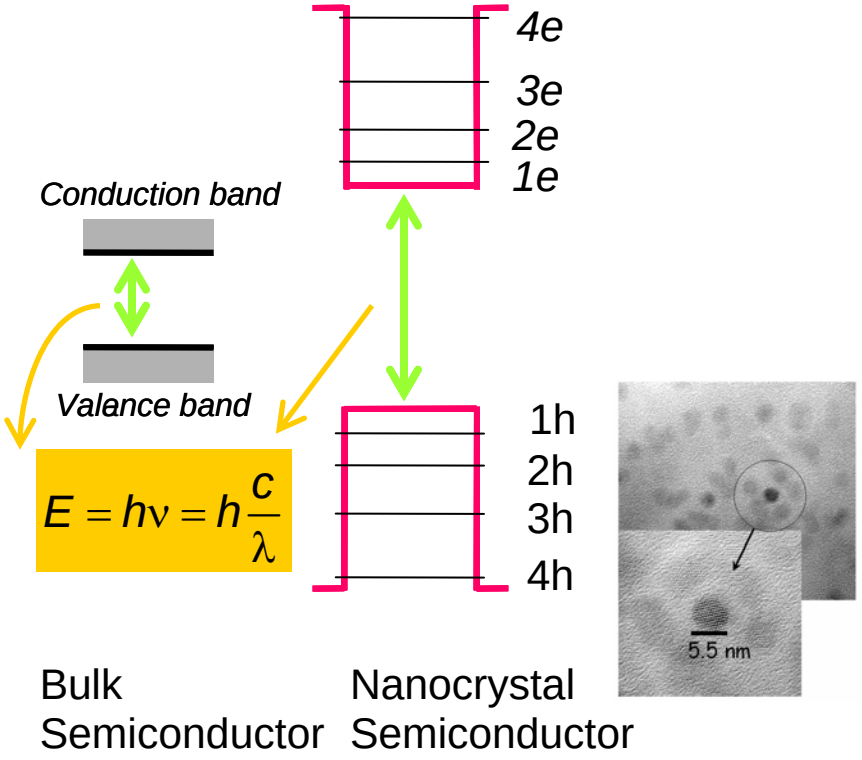

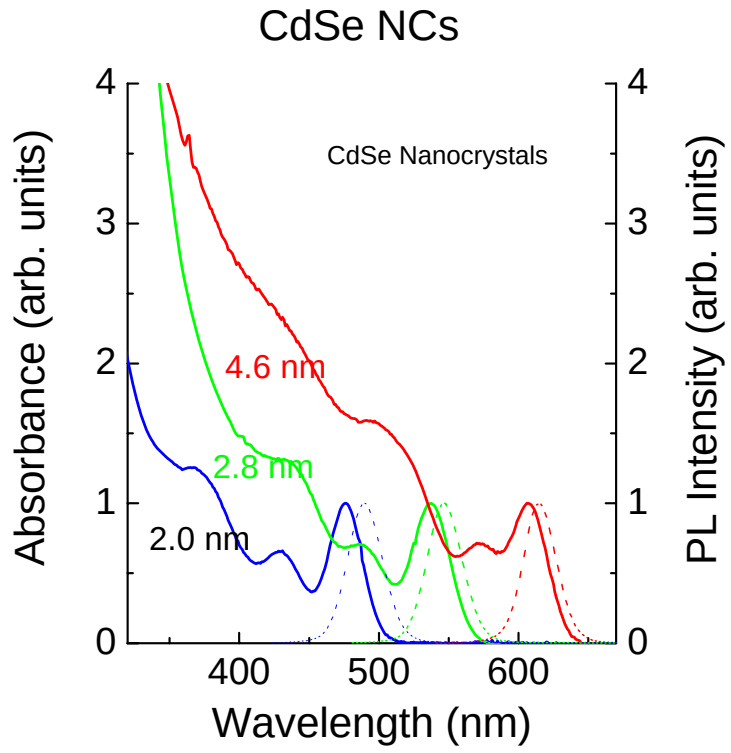

- Strong blue-shift of optical bandgap
  - Bulk: CdTe (E_g ~ 863 nm), CdSe (E_g ~ 714 nm), and CdS (E_g ~ 513 nm)
- Confinement of electrons in dot boundary
  - Atomic-like discrete energy states (multiple absorption peaks)
  - Bulk crystals: continuous energy states
- Surface effects of many atomic vacancies and defects on the surfaces in the different local environments
- Quantum confinement and surface effects modify
  - Optical absorption, photoluminescence
  - Nonlinear Optical Properties

Confinement Energy States at the Conduction-band

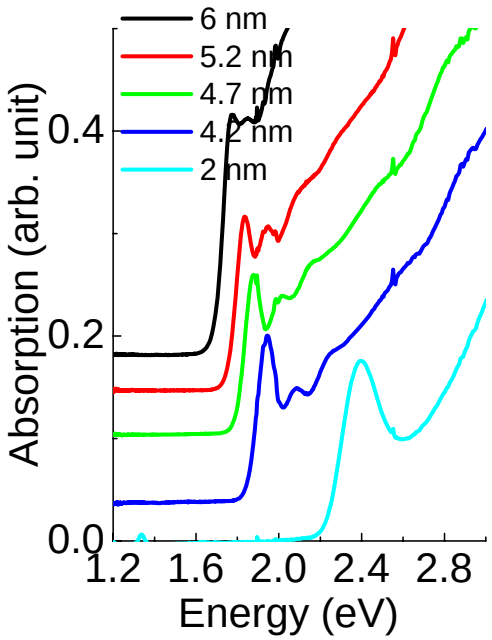

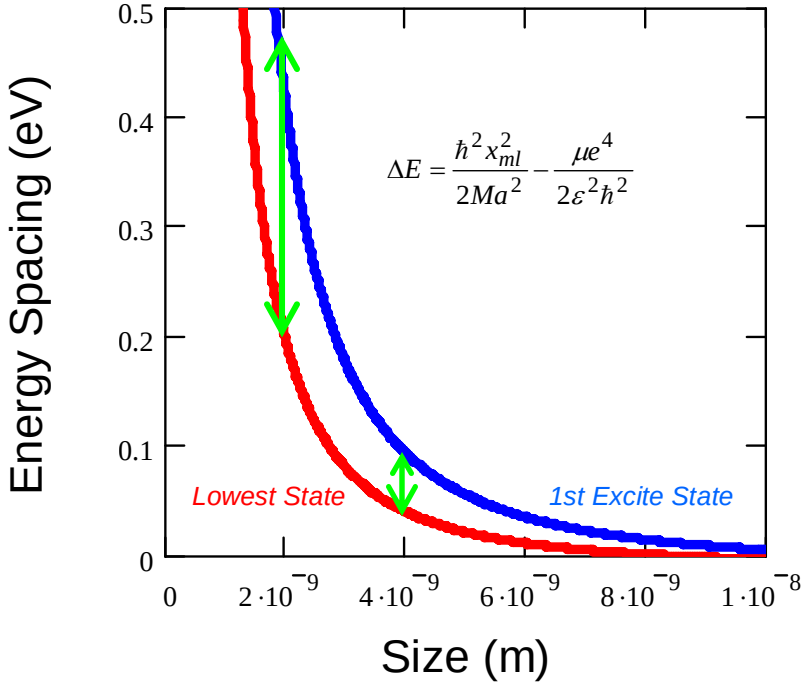

- With weak confinement

$$E_{nml} = E_g - \frac{e^2}{2\varepsilon\alpha_B n^2} + \frac{\hbar^2 x_{ml}^2}{2Ma^2}, \quad (a \geq \alpha_B)$$

- With strong confinement

$$E_{ml} = E_g - 1.786\frac{e^2}{\varepsilon a} + \frac{\hbar^2 x_{ml}^2}{2Ma^2}, \quad (a << \alpha_B)$$

  - *n*: internal exciton states arising from the e-h Coulomb interaction
  - *m, l*: states connected with the CM motion in the presence of the external potential barrier.
  - Ref.: S. Gaponenko, Nanoscale linear and nonlinear optics, edited by M Bertolotti, er al.

- Plotting with weak confinement model
- For bigger than ~4 nm quantum dot size

→Energy spacing 1st & 2nd ab. peaks: less than 50 meV

- For ~ 2 nm quantum dot size
  - → Energy spacing: more than a couple of hundred meV
  - → No 2nd peak of ex. ab. are shown in the limited sp. re.

- α_B (CdTe) ~7 nm, α_B (CdSe) ~5.6 nm, α_B (CdS) ~1.8 nm

Introduction of Nonlinear Spectroscopy

- Z-scan Spectroscopy
  - Sign and Magnitude of Nonlinear Absorption (SA or RSA) and Nonlinear Refraction
- Four Wave Mixing
  - Magnitude of Nonlinearity, Identification of Nonlinearity Order, Hyperpolarizability, Polarization- and Temperature-resolved Nonlinearity
- Nonlinear Transmittance Spectroscopy (*I-scan*)
  - Development of Saturable Absorbers
  - Development of Optical Power Limiters

Induced Polarization to Electric Field

$$P = \varepsilon_o \left(\chi^{(1)} E + \chi^{(2)} E^2 + \chi^{(3)} E^3 + \ldots \right)$$

$$\chi = \alpha + \beta^h E + \gamma^h E^2 + \ldots..$$

- First term, $\chi^{(1)}E$:
  - linear absorption & emission
- Second term, $\chi^{(2)}EE$:
  - 2nd order nonlinearity
    - Frequency doubling
    - Frequency sum/difference generation
    - Pockels cell effect
- Third term, $\chi^{(3)}EEE$:
  - 3rd order nonlinearity
    - 3rd harmonic generation
    - Raman Scattering
    - **Self focusing or defocusing**
    - Optical Phase Conjugation

- P: induced polarization of medium
- ε_0: dielectric constant of vacuum
- E: electric field
- $\chi^{(i)}$: succeptibility of i^{th} order

$$\chi^{(3)} = Re\,\chi^{(3)} + i\,Im\,\chi^{(3)}$$

$$Re\,\chi^{(3)} = \frac{4}{3} n_0^2 \varepsilon_0 c \cdot \gamma$$

$$Im\,\chi^{(3)} = \frac{1}{3\pi} n_0^2 \varepsilon_0 c \cdot \lambda\beta$$

$$\left|\chi^{(3)}\right| = \sqrt{\left(Re\,\chi^{(3)}\right)^2 + \left(Im\,\chi^{(3)}\right)^2}$$

$$n = n_o + \gamma I$$

$$\alpha = \alpha_o + \beta I$$

$$\Delta\Phi_o(t) = k\gamma I_o(t) L_{eff}$$

$$\Delta\Psi_o(t) = \beta I_o(t) L_{eff} / 2$$

Expectation of Large $\chi^{(3)}$ Effect in Nanoscale Materials

- **Quantum confinement and size effects**
  - Bandgap blue-shift with smaller size
  - Creation of discrete energy states

- **Surface effects**
  - by many atomic vacancies and defects on the surfaces in the different local environments
  - Longer lifetime at the surface trapped state
  - Strong surface plasmon resonance (Nanometals)

- **Possible inversion symmetry of nanoscale materials**
  - Non/weak $\chi^{(2)}$ effect by center of inversion symmetry
  - Even-order NL susceptibility is forbidden for inversion symmetry
    - With symmetry inversion; E → -E, P → -P:

$$-P = \varepsilon_o \chi^{(2)}(-E)(-E) = P \rightarrow P = 0 \quad \left(\chi^{(2m)} = 0\right)$$

  - like isotropic gases, liquids, and crystals of symmetry class 432
  - Nonlinear susceptibility of nanoscale materials:

$$P = \varepsilon_o \left(\chi^{(1)}E + \chi^{(2)}E^2 + \chi^{(3)}E^3 \ldots\right)$$

$$\chi = \chi^{(1)} + \chi^{(3)}E^2 + \chi^{(5)}E^4 + \ldots$$

Z-scan Nonlinear Spectroscopy

- Allows determination of both sign and magnitude of nonlinearity
- Simple nonlinear spectroscopy technique using a single Gaussian beam
- Transmittance depending on the sample z-position with respect to the focal plane of beam propagation
- Transformation of the phase distortion to the amplitude distortion for a beam propagating through a nonlinear medium

- Problems
  - Scattering effects to the open and closed Z-scan signals?
  - Induced thermal effects with long scanning time (~several minutes) or high repetition pulse excitation
    - More serious problems with thermally sensitive materials
  - Difficulty with temperature-resolved nonlinearity spectroscopy

Nonlinear Z-scan Spectroscopy

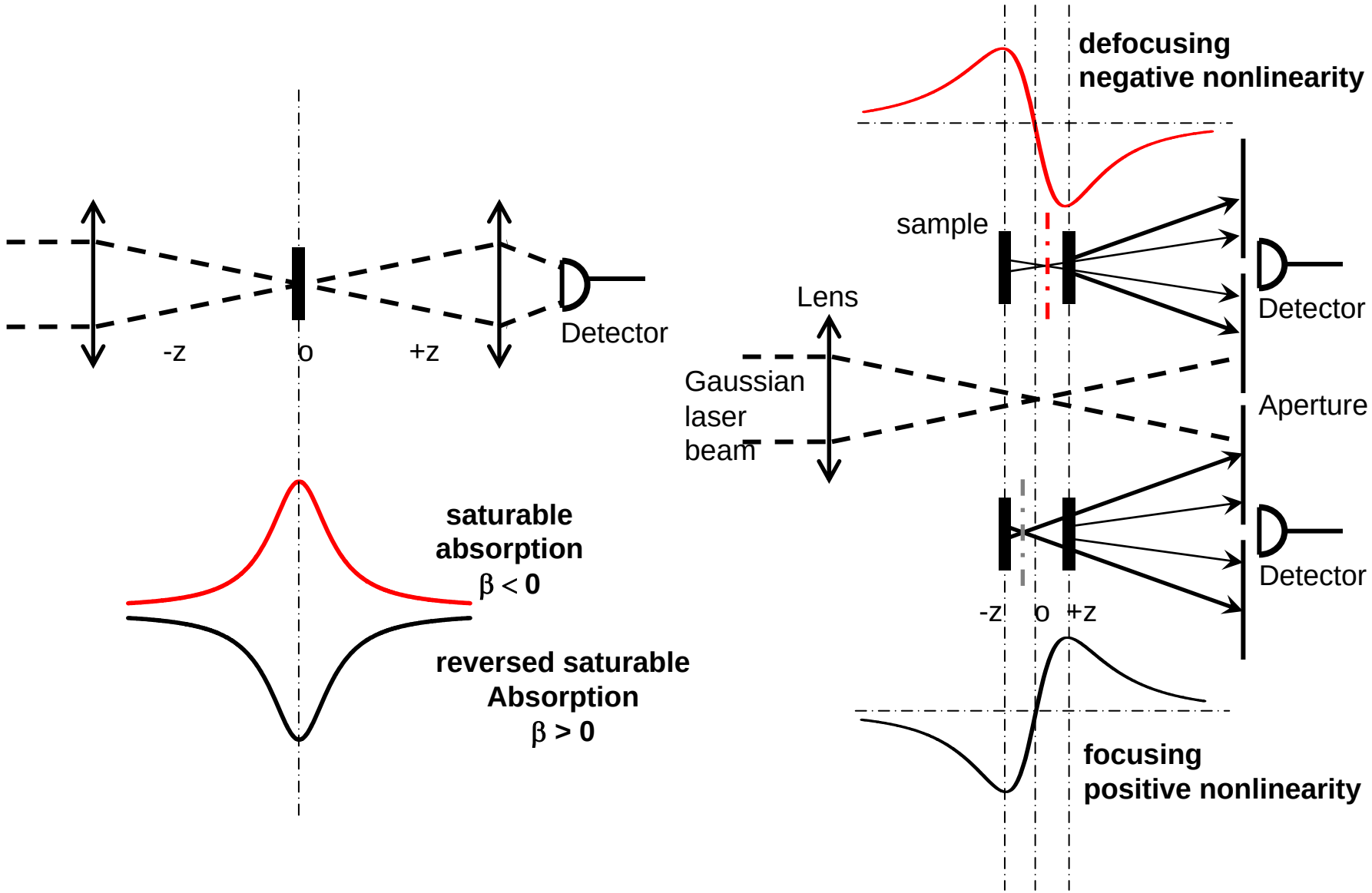

Closed Z-scan Spectroscopy

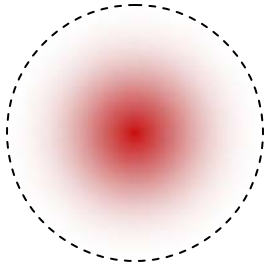

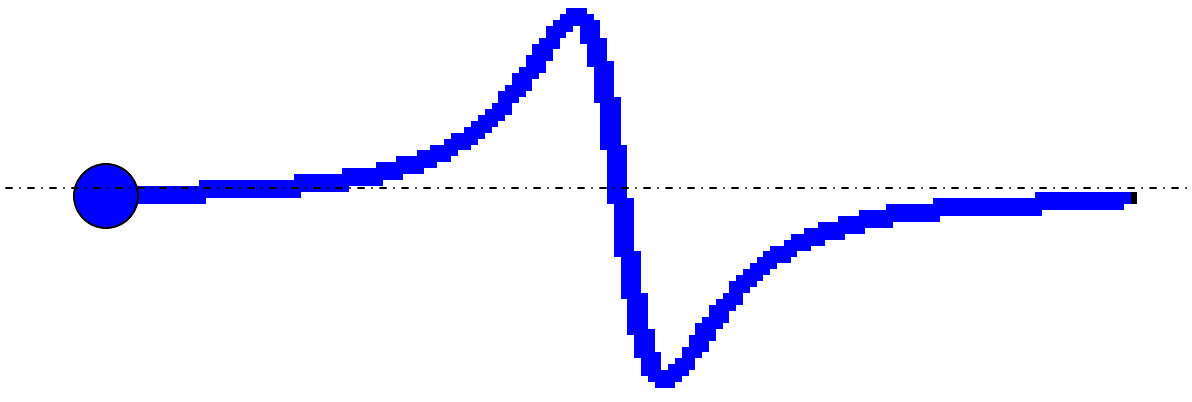

Nonlinear Transmittance for Open & Closed Z-scan Spectroscopy

- **Using the nonlinear transmittance**

$$T = \frac{\int_{-\infty}^{\infty} P_T(t)dt}{S\exp(\alpha L)\int_{-\infty}^{\infty} P_I(t)dt}$$

$P_I(t) = \pi w_o^2 I_o(t)/2$: incident power

$P_T(t) = c\varepsilon_o n_o \pi \int_o^{r_a} |E_a(r,t)|^2 r dr$: transmitted power

$S = 1 - exp\left(-2r_a^2 / w_a^2\right)$: linear transmittance of the aperture for a Gaussian input beam

- **Open Z-scan (S=1) Spectroscopy**

$$T(z, S=1) = \sum_{m=0}^{\infty} \frac{\left(\frac{-q}{1+z^2/z_o^2}\right)^m}{(m+1)^{3/2}}$$

$q(r,z,t) = \beta I(r,z,t) L_{eff}, \quad q < 1$

$L_{eff} = \left(1 - e^{-\alpha L}\right)/\alpha$: effective length

$z_o = k w_o^2 / 2$: Rayleigh length, w_o: beam radius at focus

- Fitting this equation to the experiment data → estimate the nonlinear absorption β

- **Closed Z-scan (S<<1) Spectroscopy**

$$T_{ra}(z, S<<1) = 1 - \frac{4\Delta\Phi_o x + q(3+x^2)}{(1+x^2)(9+x^2)} - \frac{4\Delta\Phi_o^2(5-3x^2) - 8\Delta\Phi_o q x(9+x^2) - q^2(40+17x^2+x^4)}{(1+x^2)(9+x^2)(25+x^2)}$$

$$\Delta\Phi_o(t) = k\gamma I_o(t) L_{eff}, \; \Delta\Psi_o(t) = \beta I_o(t) L_{eff}/2, \; x = -\left(\frac{1}{z_o}\right)\left(z + \frac{z_o^2 + z^2}{d - z}\right) \sim -\frac{z}{z_o}, \; for \; d >> z_o$$

d: propagation distance from the sample to the aperture plane

- Sensitivity of $\Delta T_{P\text{-}V}$ increases for smaller linear transmittance of the aperture S for same $\Delta\Phi_o$
- Fitting this equation to the experiment data →estimate both nonlinear refraction γ and NLA β

Ref.: 1. J.T. Seo, and et. al., phys. stat. sol. (c), 1(4), 771 (2004). 2. J.T. Seo, and et. al., Applied Physics Letters, 82(25), 4444 (2003).

Resonant and Non-resonant Optical Nonlinearity

- Resonant nonlinearity
  - Relatively slow response
  - Two-step absorption
  - Relatively large nonlinearity
- Nonresonant nonlinearity
  - Relatively fast response
  - Two-photon absorption

- Reverse saturable absorption
  - Positive nonlinear absorption ($\beta>0$)
  - ESA > GSA
- Saturable absorption
  - Negative nonlinear absorption ($\beta<0$)
  - ESA < GSA

Z-scan spectroscopy of CdSe Q-dots in Toluene with resonant Excitation

Resonant excitation
with 8-ns pulse width at 532 nm

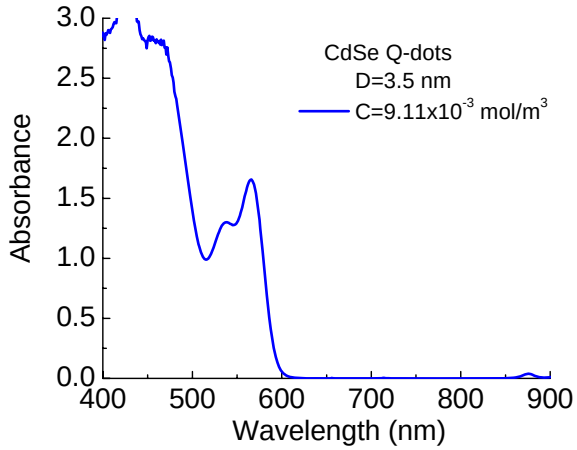

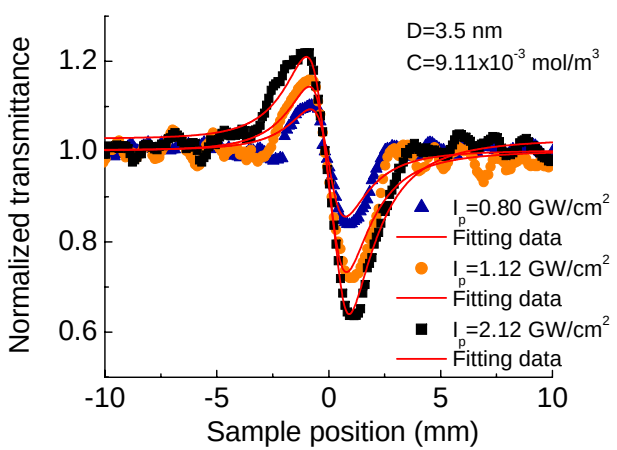

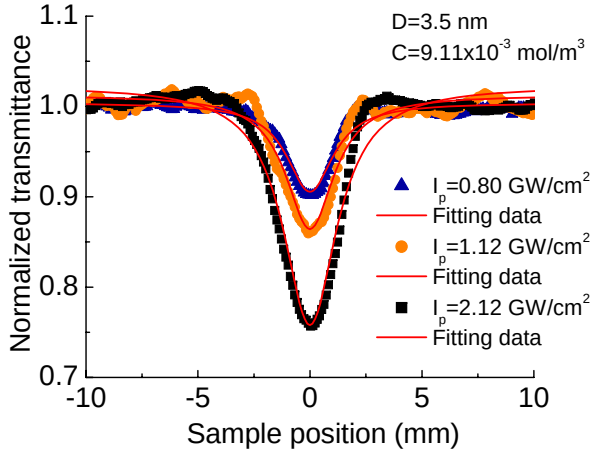

- Average size of CdSe Q-dots: ~3.5 nm.
- First absorption peak: ~565 nm
- Excitation for nonlinear spectroscopy:
  - Resonant excitation at 532 nm, 8 ns, 10 repetition rate
- Concentration of CdSe Q-dots: ~9.11×10^{-3} mol/m^3
- Peak intensity for nanosecond & nonresonant excitation: ~0.8 – 2.12 GW/cm^2
- Nonlinear refraction
  - Negative Polarity (Self-defocusing)
  - Magnitude: γ ~ -1.94×10^{-17} m^2/W
- Nonlinear absorption
  - Magnitude: β ~ 6.50×10^{-11} m/W
  - Two step absorption

Z-scan Spectroscopy of Toluene

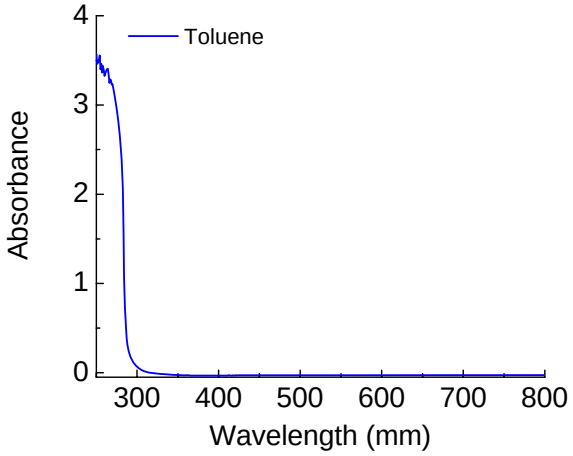

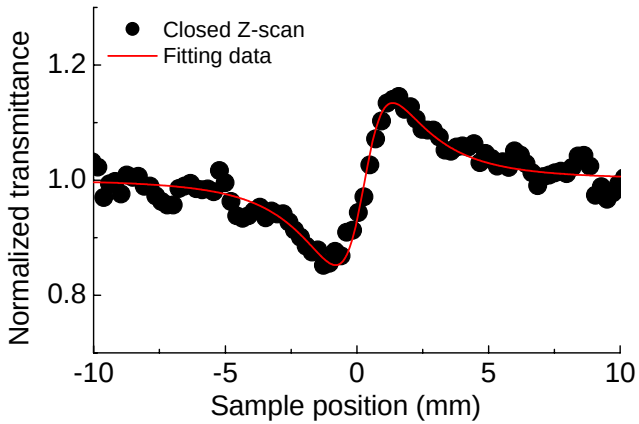

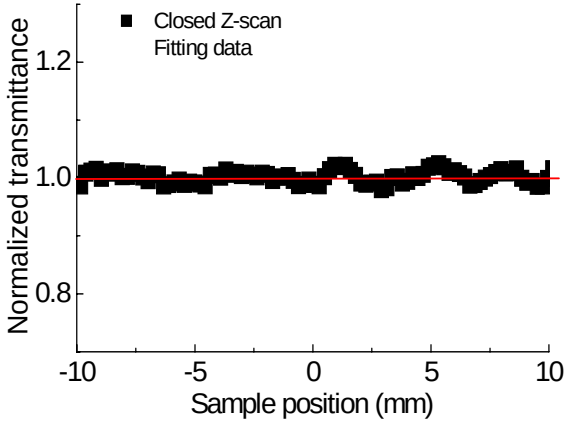

- Peak intensity for nanosecond & nonresonant excitation: ~2.12 GW/cm^2
- Nonlinear refraction
  - Positive Polarity (Self-focusing)
  - Magnitude: $\gamma \sim 4.85\times10^{-18}$ m^2/W
- Nonlinear absorption
  - Magnitude: $\beta \sim 0$ m/W
  - Highly nonlinear refractive materials at the laser intensity level of ~2.12 GW/cm^2

Effective Third-order Optical Nonlinearity of CdSe Q-dots

Resonant excitation
with 8-ns pulse width at 532 nm

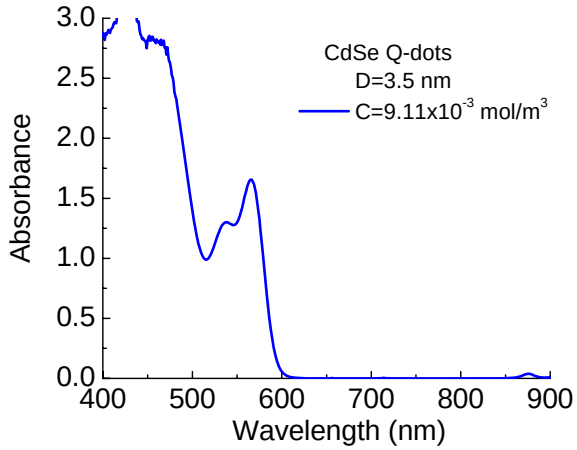

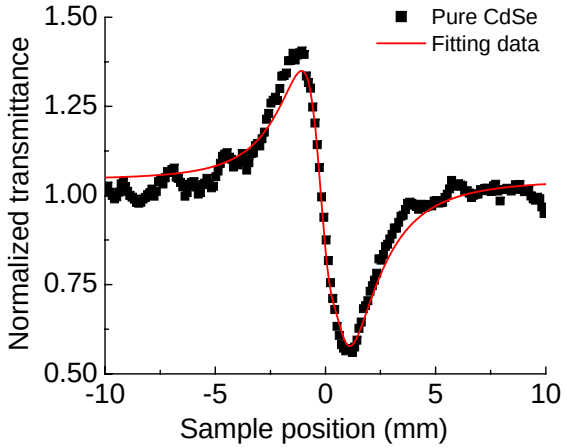

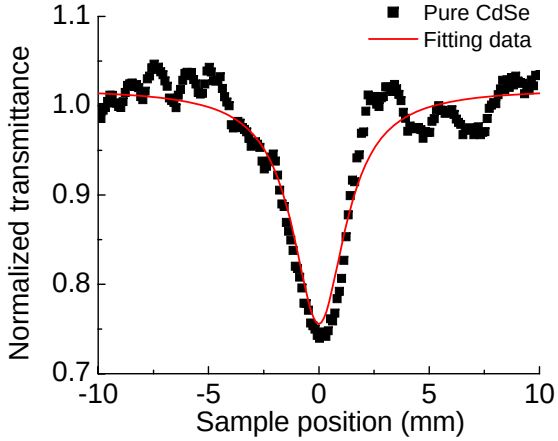

- Average size of CdSe Q-dots: ~3.5 nm.
- First absorption peak: ~565 nm
- Excitation for nonlinear spectroscopy:
  - Resonant excitation at 532 nm, 8 ns, 10 repetition rate
- Peak intensity for nanosecond & resonant excitation: ~2.12 GW/cm^2
- Nonlinear refraction
  - Negative Polarity (Defocusing)
  - Nonlinear refraction polarity of CdSe Q-dots in toluene
  - Magnitude: $\gamma \sim -9.55\times10^{-18}$ m^2/W
- Nonlinear absorption
  - Magnitude: $\beta \sim 4.49\times10^{-11}$ m/W
  - Two step absorption
- 3rd-order nonlinear susceptibility: $|\chi^{(3)}| \sim 1.89\times10^{-19}$ m^2/V^2 (~1.35×10^{-11} esu)

$$\left|\chi^{(3)}\right| = \left[\left(\mathrm{Re}\,\chi^{(3)}\right)^2 + \left(\mathrm{Im}\,\chi^{(3)}\right)^2\right]^{\frac{1}{2}}$$

$$\text{where } \mathrm{Re}\,\chi^{(3)} = \frac{4}{3} n_{CdSe}^2 \varepsilon_0 c \cdot \gamma, \text{ and } \mathrm{Im}\,\chi^{(3)} = \frac{1}{3\pi} n_{CdSe}^2 \varepsilon_0 c \lambda \cdot \beta$$

$$n_{CdSe} = \sqrt{1 + \frac{\left(\varepsilon_{bulk} - 1\right)}{1 + \left(\frac{0.75}{D}\right)^{1.2}}}$$

$$\text{where } \varepsilon_{bulk} \cong 6.2, \; D \text{ is the size of the QDs}$$

Effective Nonlinear Absorption and Refraction Coefficients of CdSe Nanocrystals

Nonresonant excitation at 775 nm with 150-fs pulse width

Femtosecond Nonresonant

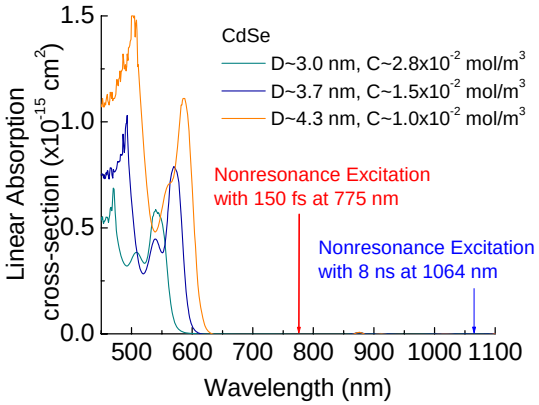

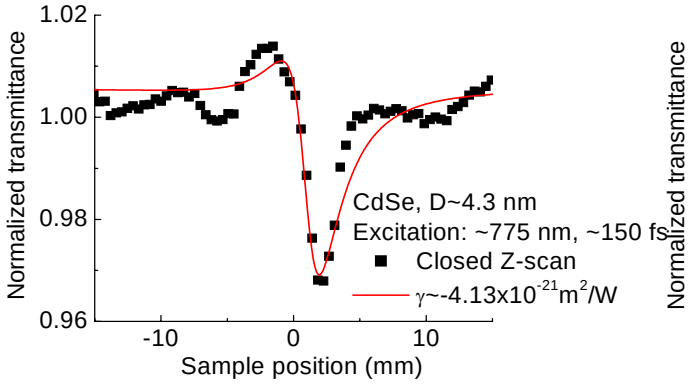

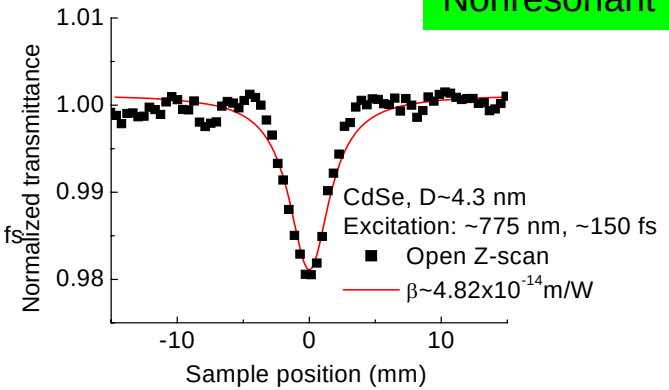

Resonant excitation at 532 nm with 8-ns pulse width

Nanosecond Resonant

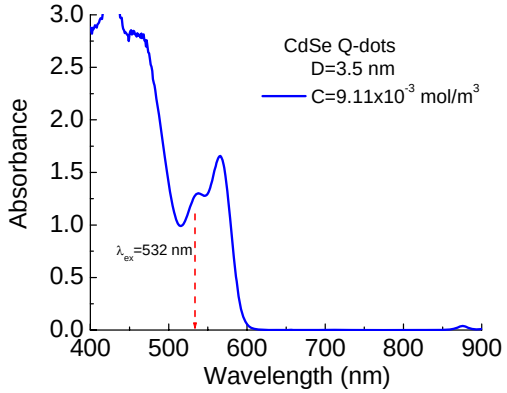

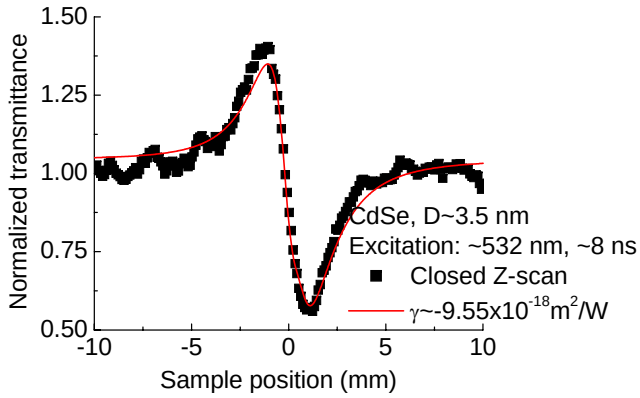

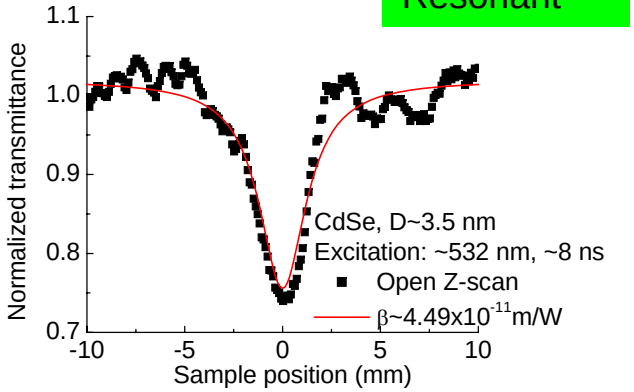

- Lager nonlinearity with resonant & longer pulse excitation
  - Two-step absorption is much stronger than two-photon absorption
  - Existences of multiple NL processes in longer pulse width

Four-Wave Mixing (FWM)

- Magnitude of nonlinearity
- Identification of nonlinearity Order
- Hyperpolarizability by investigating concentration-resolved nonlinearity
- Polarization-resolved nonlinearity
- Temperature-resolved nonlinearity

- Problems
  - No sign of nonlinearity
  - No indication of nonlinear absorption or refraction
  - No information of sample position for optical power limiter development

Concept of Forward Degenerate Four-Wave Mixing

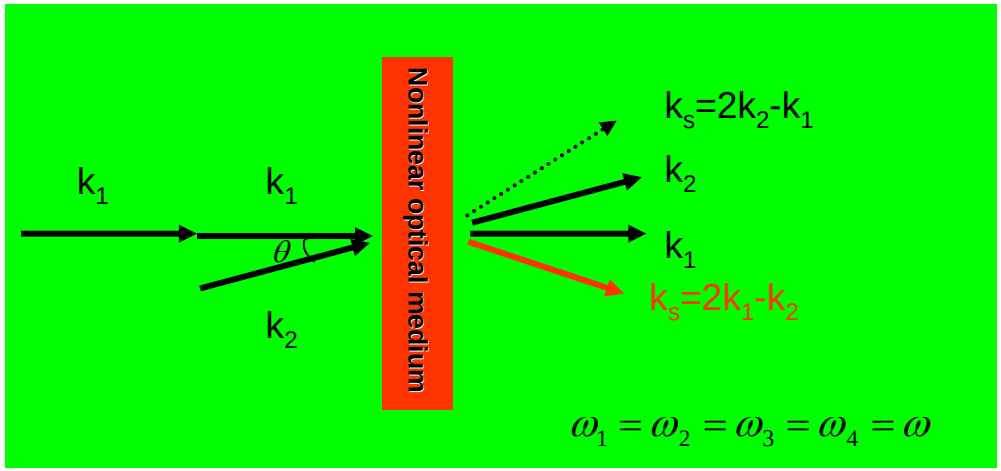

- k_1: Strong pump beam
- k_2: Weak probe beam
- Creation of dynamic grating in the sample by k_1 and k_2 interaction
- Diffraction of k_1 by the grating creates the signal of FWM
- Signal beam: $2k_1-k_2 > 2k_2-k_1$ → Nonlinearity information of sample
- Signal Intensity $I_s=aI_t^3$ →cubic nonlinearity

Magnitude of Nonlinearity by Four-Wave Mixing

- Nonresonance excitation

$$\chi_S^{(3)} = \sqrt{\frac{I_S}{I_R}}\left(\frac{n_S}{n_R}\right)^2\left(\frac{L_R}{L_S}\right)\chi_R^{(3)}$$

- Resonance excitation [a)]
  - Sample condition: $\alpha L<1$

$$\chi_S^{(3)} = \sqrt{\frac{I_S}{I_R}}\left(\frac{n_S}{n_R}\right)^2\left(\frac{L_R}{L_S}\right)\left(\frac{\alpha L}{e^{-\alpha L/2}\left(1-e^{-\alpha L}\right)}\right)\chi_R^{(3)}$$

- Reference Sample (CS_2)
  - Reference thickness: L~1.0 mm
  - Linear refractive index: n ~1.63 [b)]
  - $\chi^{(3)}{}_{ref}$=~9.5×10^{-21} m^2/V^2 at 532 nm and 8 ns [c)]
- References

a) X. Zhan, Y. Liu, D. Zhu, X. Liu, G. Xu, and P. Ye, “Large third-order nonlinear optical response of a conjugated copolymer consisting of 2,5-diethynylthiophene and carbazole units”, Chem. Phys. Lett., 343, 493 (2001).

b) B. Illine, K. Evain, and M. L. Guennec, “A way to compare experimental and SCRF electronic static dipole polarizability of pure liquids”, J. Mol. Struct. (Theochem) 630, 1 (2003).

c) P. Wang, H. Ming, J. Xie. W. Zhang, X. Gao, Z. Wu, and X. Wei, “Substituents effect on the nonlinear optical properties of C60 derivatieves”, Opt. Comm. 192, 387 (2001).

Investigation of Hyperpolarizability by Concentration-resolved FWM

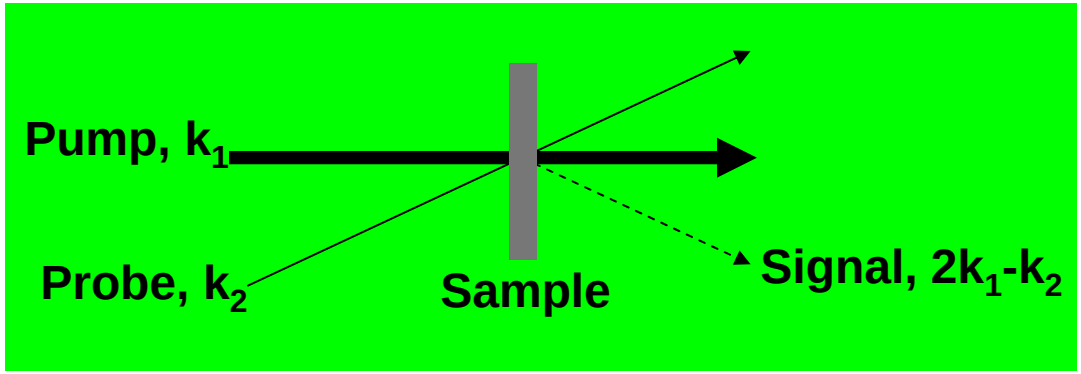

- Third-order nonlinearity with a reference material

$$\chi_S^{(3)} = \sqrt{\frac{I_S}{I_R}}\left(\frac{n_S}{n_R}\right)^2\left(\frac{L_R}{L_S}\right)\chi_R^{(3)}, \quad \chi_S^{(3)} = \sqrt{\frac{I_S}{I_R}}\left(\frac{n_S}{n_R}\right)^2\left(\frac{L_R}{L_S}\right)\left(\frac{\alpha L}{e^{-\alpha L/2}\left(1-e^{-\alpha L}\right)}\right)\chi_R^{(3)}$$

- Concentration-resolved third-order nonlinearity

$$\chi^{(3)} = f^4 N_a \langle \gamma^h \rangle C = (slope) C$$

- Hyperpolarizability

$$\langle \gamma^h \rangle = \frac{slope}{f^4 N_a}, \qquad f = \frac{3n_{matrix}^2}{\tilde{n}_{sample}^2 + 2n_{matrix}^2}$$

- Unit conversions

$$\chi^{(3)}\left[\frac{m^2}{V^2}, SI\right] = \frac{4\pi \times 10^{-8}}{9}\chi^{(3)}[esu], \quad \langle \gamma^h \rangle\left[\frac{m^5}{V^2}, SI\right] = \frac{4\pi \times 10^{-14}}{9}\langle \gamma^h \rangle[esu]$$

Polarization-resolved FWM

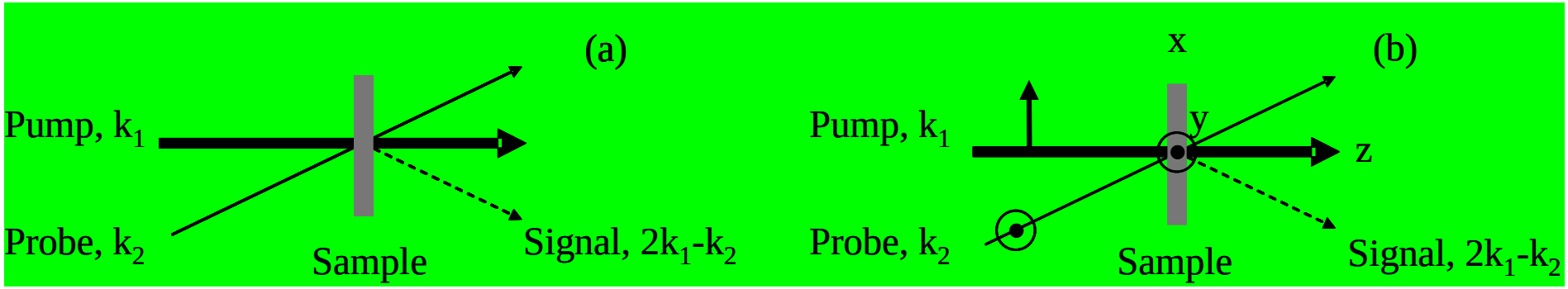

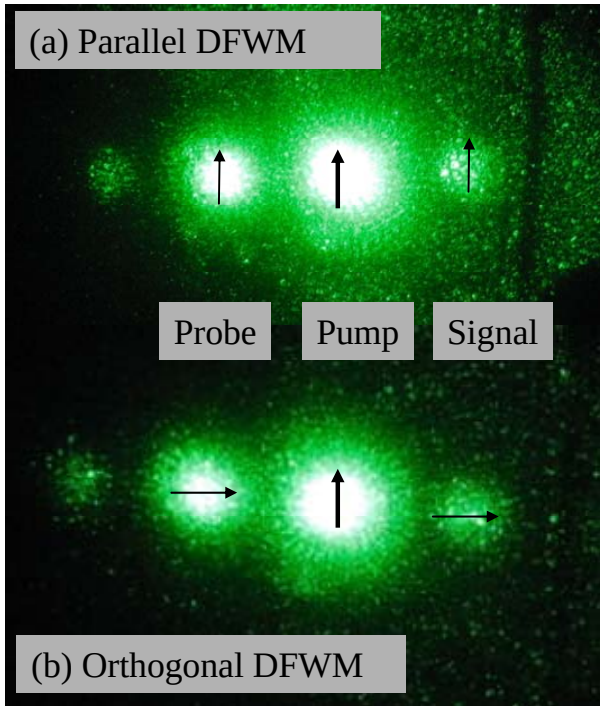

- Macroscopically isotropic media
  - Electronic polarization process

$$\chi^{(3)}_{xxxx} = \chi^{(3)}_{xxyy} + \chi^{(3)}_{xyxy} + \chi^{(3)}_{xyyx}$$

$$\frac{1}{3} = \frac{\chi^{(3)}_{xyyx}}{\chi^{(3)}_{xxxx}} = \frac{\chi^{(3)}_{xyxy}}{\chi^{(3)}_{xxxx}} = \frac{\chi^{(3)}_{xxyy}}{\chi^{(3)}_{xxxx}}$$

  - Molecular reorientation

$$\frac{3}{4} = \frac{\chi^{(3)}_{xyyx}}{\chi^{(3)}_{xxxx}} = \frac{\chi^{(3)}_{xyxy}}{\chi^{(3)}_{xxxx}}, \quad \frac{1}{2} = \frac{\chi^{(3)}_{xxyy}}{\chi^{(3)}_{xxxx}}$$

  - Thermal or Intensity grating

$$0 = \frac{\chi^{(3)}_{xyyx}}{\chi^{(3)}_{xxxx}} = \frac{\chi^{(3)}_{xyxy}}{\chi^{(3)}_{xxxx}} = \frac{\chi^{(3)}_{xxyy}}{\chi^{(3)}_{xxxx}}$$

Continued DFWM (up to third-order)

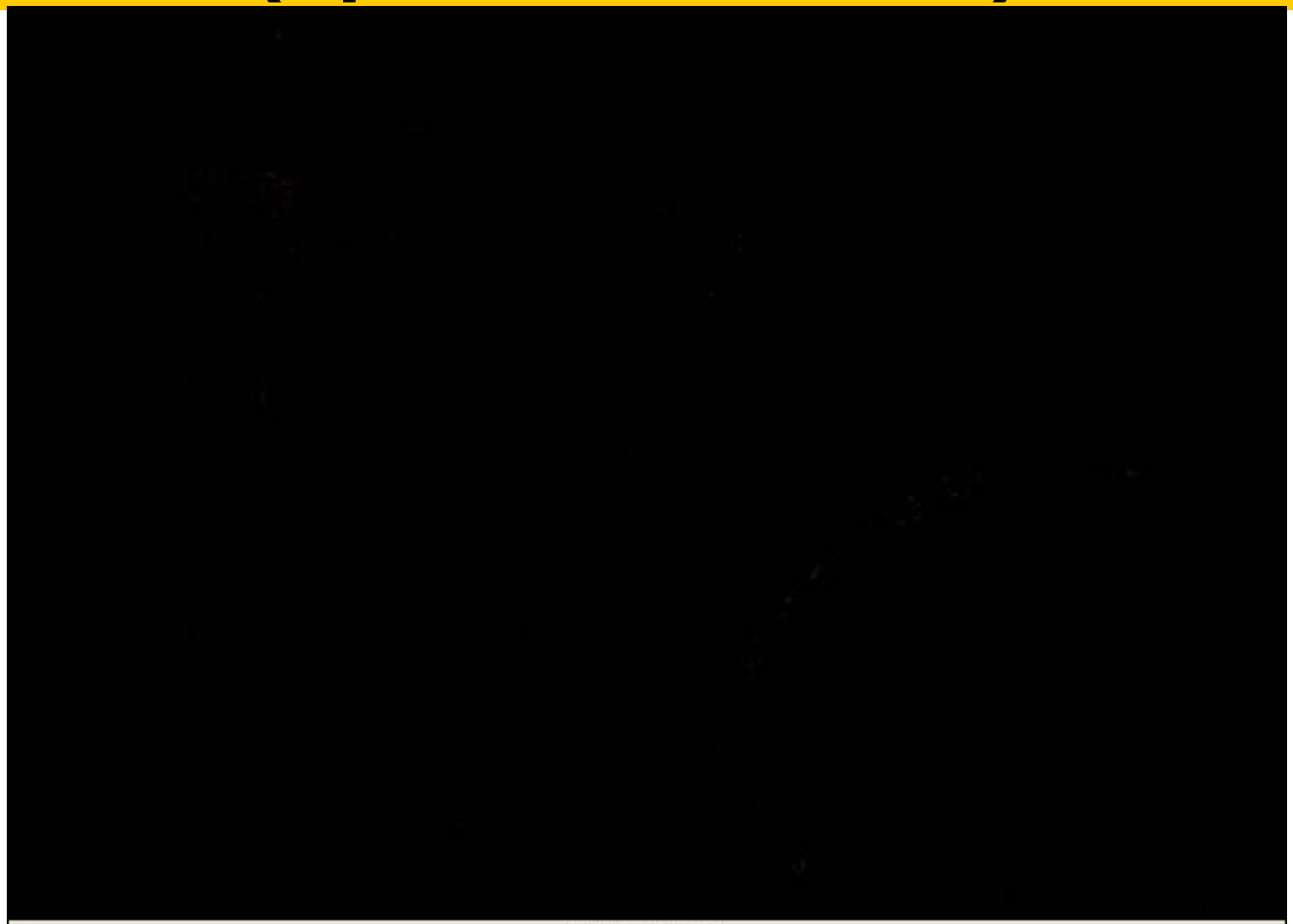

MVI_1207

Continued DFWM (up to fifth-order)

MVI_1284

Continued DFWM (up to fifth-order)

MVI_1282

Cubic Dependence Investigation of DFWM Signals of CdSe Q-Dots (~3.5 nm) with Resonant Excitation

Resonant excitation
with 8-ns pulse width at 532 nm

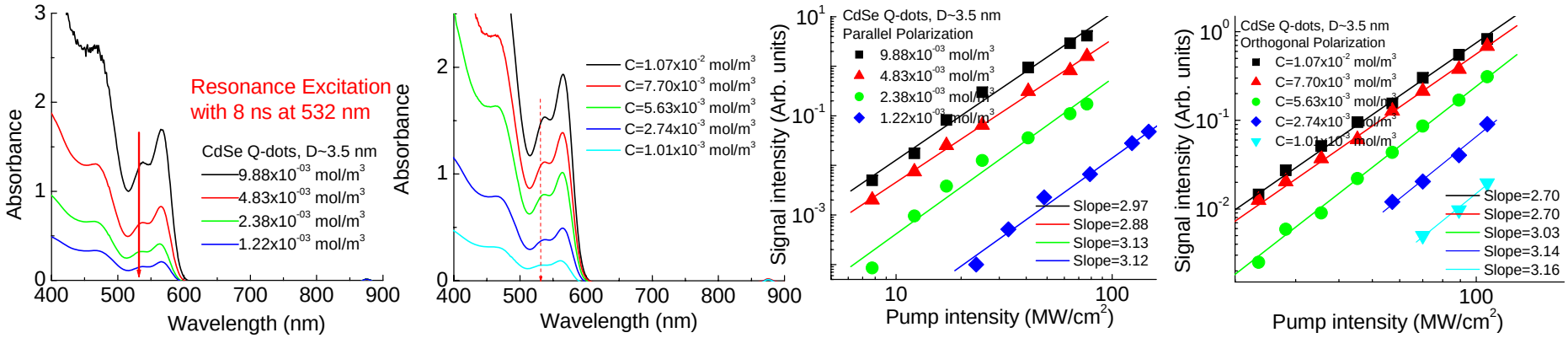

- ***Resonant excitation at 532 nm***, 8 ns, 10 repetition
- Input peak intensity level: ~10–100 MW/cm^2
- Slopes of both parallel and orthogonal polarizations: ~ 3
  - indicates dominant third-order nonlinearity

Effective $\chi^{(3)}$ of CdSe Q-Dots
with Nanosecond Resonant Excitation @532 nm

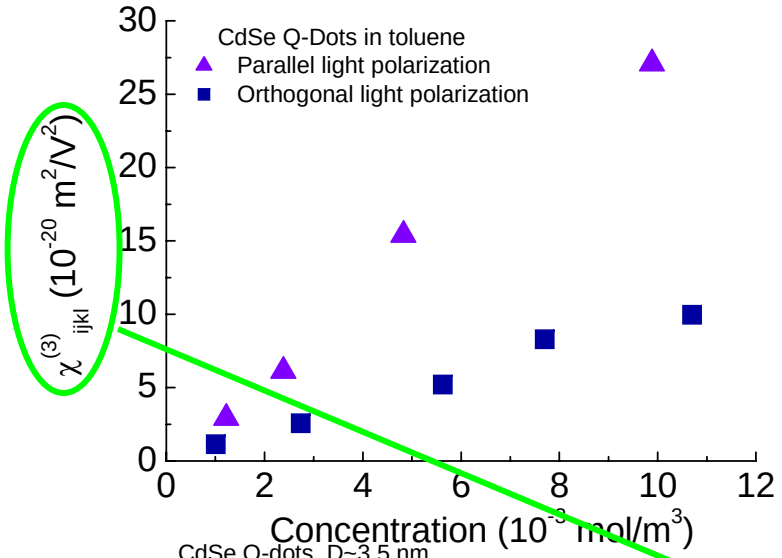

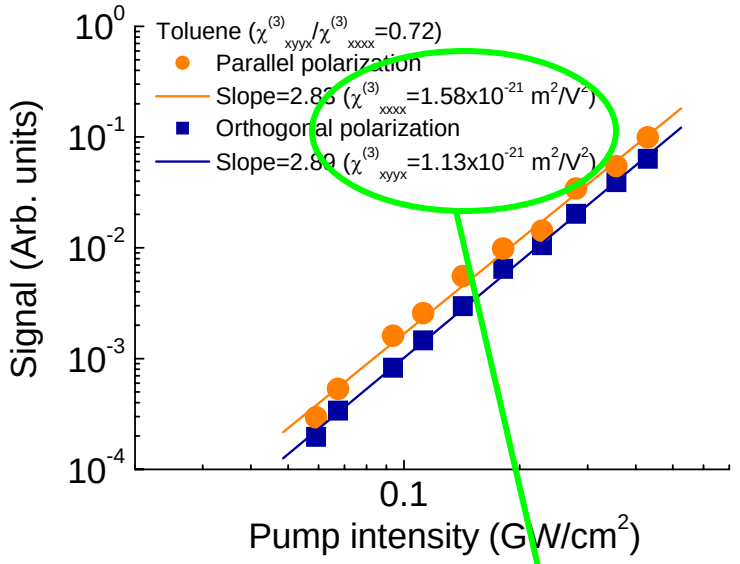

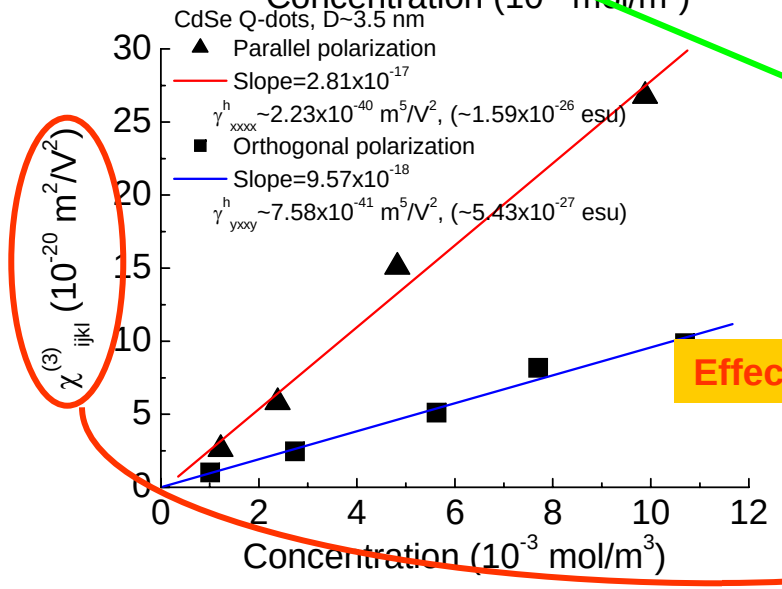

$$\chi^{(3)}_{total} = \chi^{(3)}_{CdSe\ Q-Dots\_eff} + \chi^{(3)}_{toluene}$$

Effective $\chi^{(3)}$ including the dielectric effect of QDs and toluene

Effective Resonant Third-order Nonlinearity and Hyperpolarizability of CdSe Q-Dots

Resonant excitation with 8-ns pulse width at 532 nm

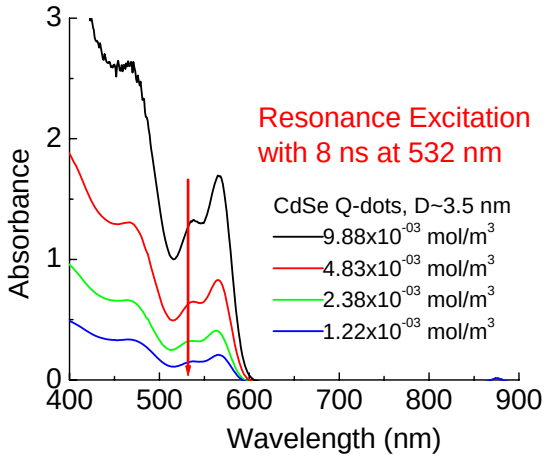

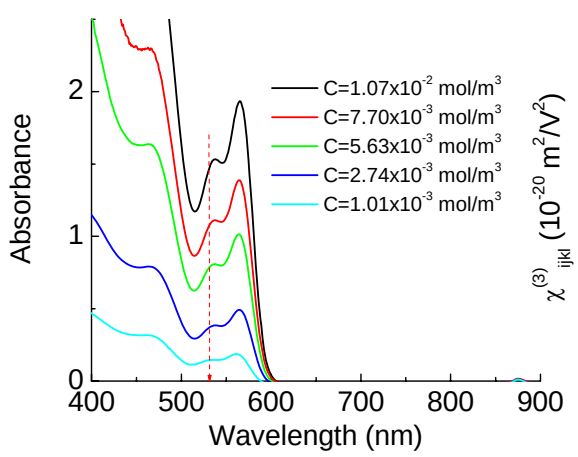

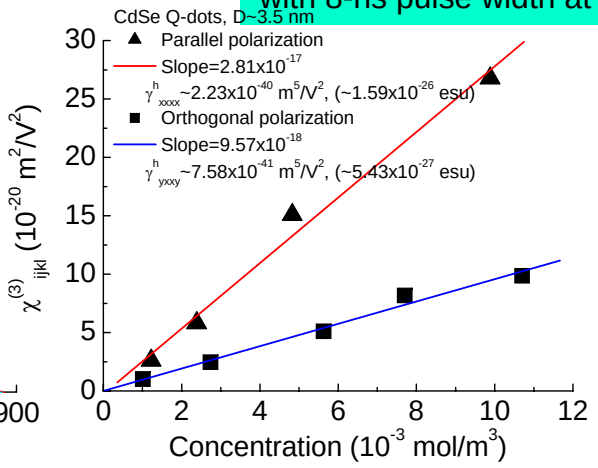

- Input peak intensity level: ~10–100 MW/cm^2
- $\chi^{(3)}$ effect of matrix (toluene) was substracted
- Hyperpolarizability
  - Parallel polarization
    - ~2.23×10^{-40} m^5/V^2 (~1.59×10^{-26} esu)
  - Orthogonal Polarization
    - ~7.58×10^{-41} m^5/V^2 (~5.43×10^{-27} esu)
- $\chi^{(3)}_{xyyx} / \chi^{(3)}_{xxxx}$~0.34: large contribution of electronic process to the $\chi^{(3)}$

Effective Nonesonant Third-order Nonlinearity and Hyperpolarizability of CdSe Q-Dots

Nonresonant excitation
with 8-ns pulse width at 1064 nm

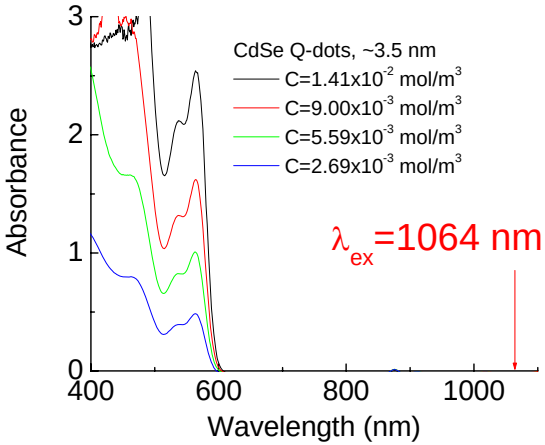

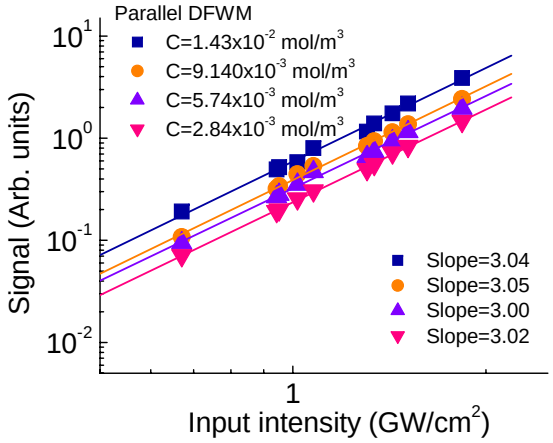

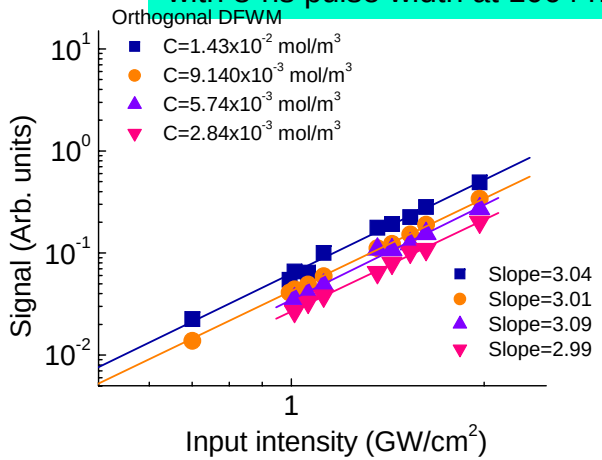

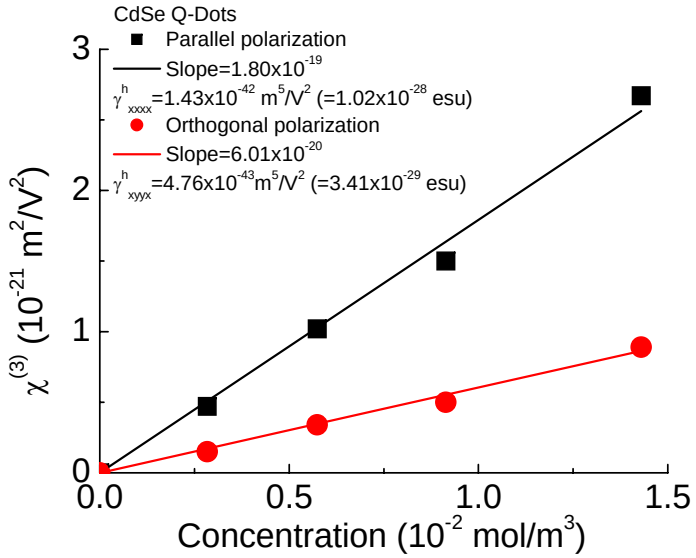

- Input peak intensity level: ~1 GW/cm^2
- Cubic dependence of signal to the input intensity → third-order nonlinearity
- $\chi^{(3)}$ effect of matrix (toluene) was substracted
- Hyperpolarizability
  - Parallel polarization
    - ~1.43×10^{-42} m^5/V^2 (~1.02×10^{-28} esu)
  - Orthogonal Polarization
    - ~4.76×10^{-43} m^5/V^2 (~3.41×10^{-29} esu)
- $\chi^{(3)}_{xyyx} / \chi^{(3)}_{xxxx}$~0.33: large contribution of electronic process to the $\chi^{(3)}$

I-scan Nonlinear Spectroscopy

- Similar as Z-scan
  - Changing input intensity instead of changing sample position
  - Sample position around the peak or the valley of Z-scan or position near the Rayleigh length
- Provides optical power limiting properties
  - Sample position near the valley of Z-scan spectroscopy
  - Transmittance depending on the input intensity
  - Phase distortion dependant on the input intensity

Nonlinear Transmittance Device (NTD) for Homeland Security and Battlefield Enhancement

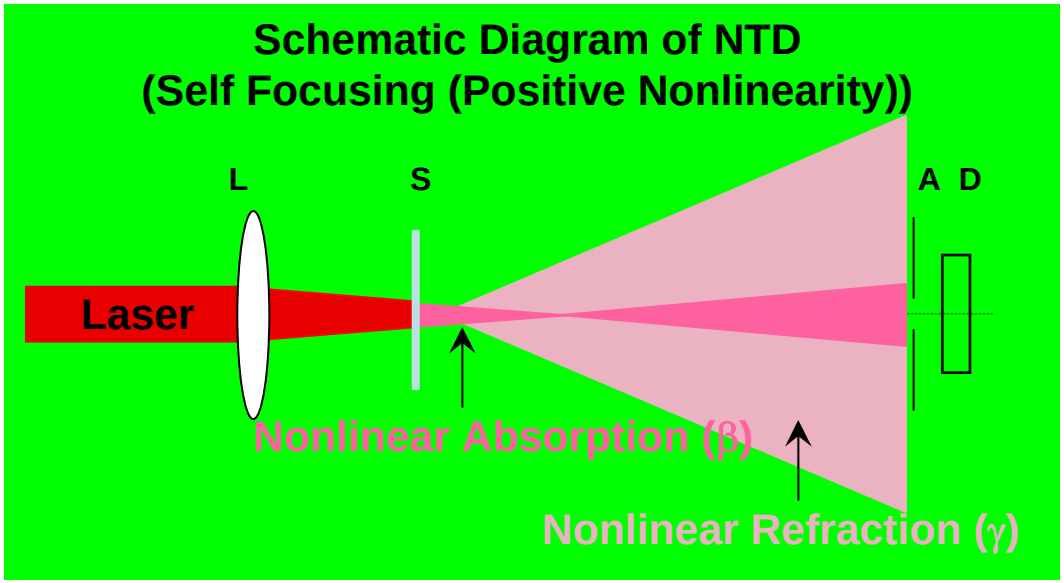

Absorption: $\alpha = \alpha_o + \beta I$

Refraction: $n = n_o + \gamma I$

Phase shift: $\Delta\Phi_o(t) = k\gamma I_o(t)L_{eff}$

$\Delta\Psi_o(t) = \beta I_o(t)L_{eff} / 2$

- **Concept of NTD**
  - As laser intensity increases
    - Total absorption, total refraction and phase shifts are increased.
    - Results in no/weak transmittance to the detector or human eye
- **Requirement of NTD**
  - High transmittance at very low intensity
  - No transmittance at high intensity
  - High Nonlinear figure of merit

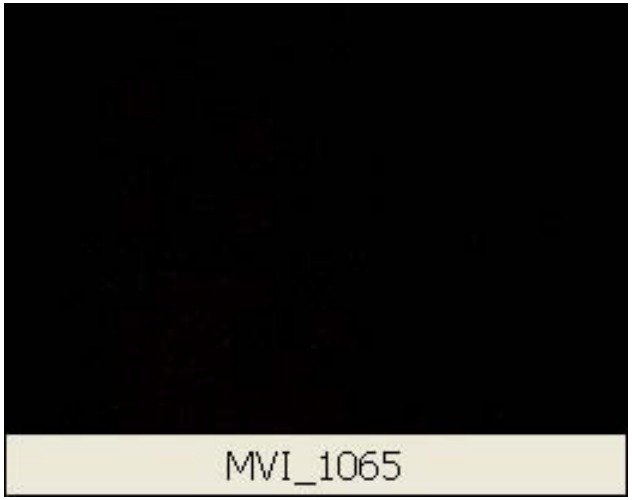

ref.: J.T. Seo, Q. Yang, S. Creekmore, D. Temple, K.P. Yoo, S.Y. Kim, A. Mott, M. Namkung, and S.S. Jung, "Large pure refractive nonlinearity of nanostructure silica," Applied Physics Letters, 82(25), 4444 (2003).

Battlefield Enhancement
- Sensor Protection -

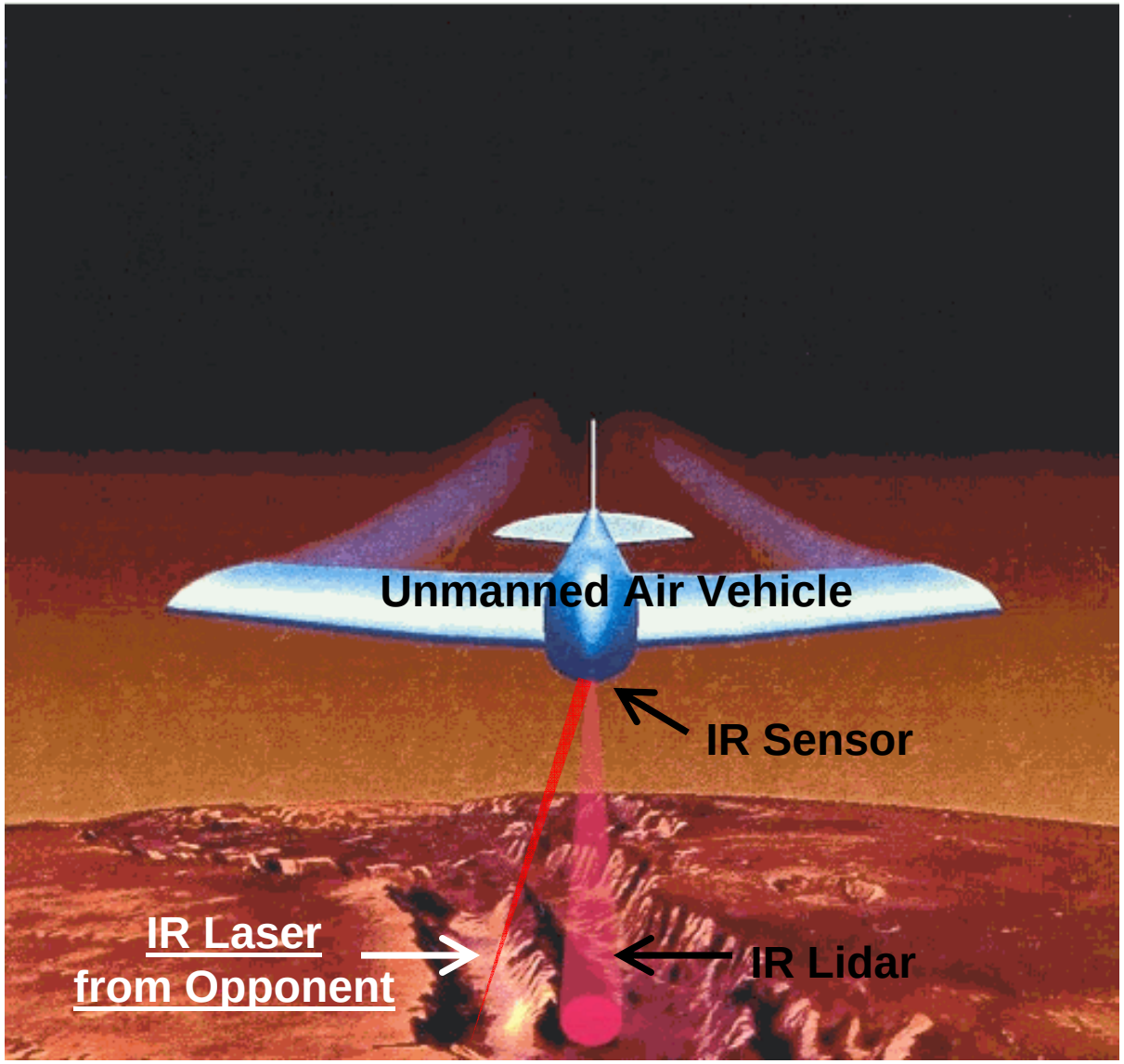

War Fighter
- Eye Protection -

Battlefield Enhancement
- Eye Protection -

Lasers from Opponents

Battlefield Enhancement
- Eye Protection -

http://www.yahoo.com Yahoo! News

FBI Probes More Lasers Shot at Airplanes

FBI and Homeland Security Department sent a memo to law enforcement agencies in Nov. 2004:

They had evidence terrorists have explored using lasers as weapons

By LESLIE MILLER, Associated Press Writer

WASHINGTON - At least a dozen cases of lasers being beamed into aircraft cockpits since Christmas are being investigated by the FBI. The lasers can temporarily blind pilots. A cluster of incidents received wide attention between Christmas and New Year's Day, and the FBI says at least four more have occurred in the past week. Authorities have continued to rule out terrorism. Transportation Secretary Norman Mineta was briefing reporters Wednesday about the issue at the Federal Aviation Administration's aeronautical research center in Oklahoma City. Mineta was expected to announce new measures for alerting pilots and preparing them to react when lasers are shined at their aircraft. He was also expected to outline ways to notify law enforcement investigators more quickly. Last week, a pilot told law enforcement officials that a green light appeared on the nose of his aircraft as it was taking off from the Burbank, Calif., airport. "To our knowledge there was no danger to the aircraft," said Cathy Viray, spokeswoman for the FBI in Los Angeles. Last weekend, two pilots near Washington Dulles International Airport reported lasers beamed at them, according to FBI spokeswoman Debra Weierman. The first incident occurred Saturday and involved a helicopter from the Fairfax County (Va.) Police Department; the other happened Sunday to a US Airways Express flight. Weierman said the bureau was investigating. There have been no arrests and neither pilot was affected by the laser light, she said. In Boise, Idaho, a pilot told the FBI that someone was possibly using a red laser on a small plane shortly after takeoff Friday evening, according to Dominic Venturi, the FBI supervisor. "It did not injure the pilot or any of the passengers on board," Venturi said, adding the FBI believes it has identified the person responsible. "We feel confident it is not related to terrorism," he said.

Beginning Christmas night, there were reports of lasers pointed at aircraft cockpits in Cleveland, Houston, Colorado Springs, Colo., Medford, Ore., and Nashville, Tenn. Many of the reports described a green beam. A New Jersey man was arrested and charged last week for aiming a green laser at a small jet flying over his home near Teterboro Airport. The man, David Banach of Parsippany, said he had been using the device to point at the stars from his back yard. That type laser pointer, which sells for $119, is the most powerful that can be used in a public place without government regulation, according to Bigha, the company that manufactures it. It produces a bright green beam that can be seen up to 25,000 feet away, and is used by bird watchers, astronomers and lecturers to point out faraway objects. The FBI and Homeland Security Department sent a memo to law enforcement agencies in November saying they had evidence terrorists have explored using lasers as weapons. An FAA report released in June found that even the lowest-intensity lasers temporarily impaired the vision of most of 34 pilots who were studied in a flight simulator.

Yahoo! News Wed, Jan 12, 2005
http://story.news.yahoo.com/news?tmpl=story&cid=514&e=4&u=/ap/20050112/ap_on_go_ot/laser_beam_aircraft

Airport Security

Airport Security

Industrial Application
- Arc Welding Mask -

Photographer: Joe Fudge, Daily Press, A8, Sunday, September 7, 2003.
A welder, Mike Eaton, at Northrop Grumman Newport News burned former President George H.W. Bush's initials into a metal plate to be affixed to the carrier.

Nonlinear Transmittance Properties of CdSe Q-dots

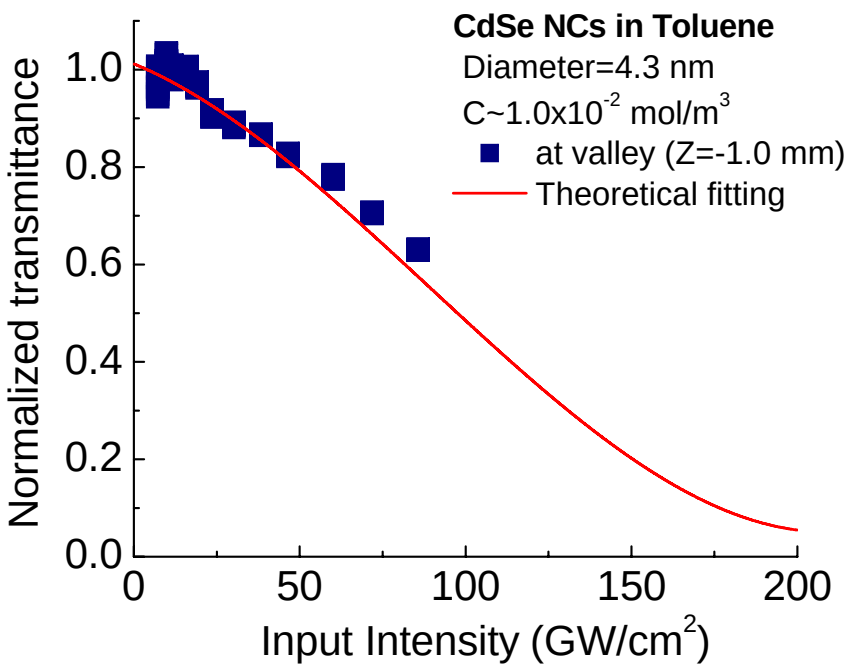

- Nonresonant Excitation with 150-fs pulse width at ~775 nm
  - Limiting threshold: ~100 GW/cm^2

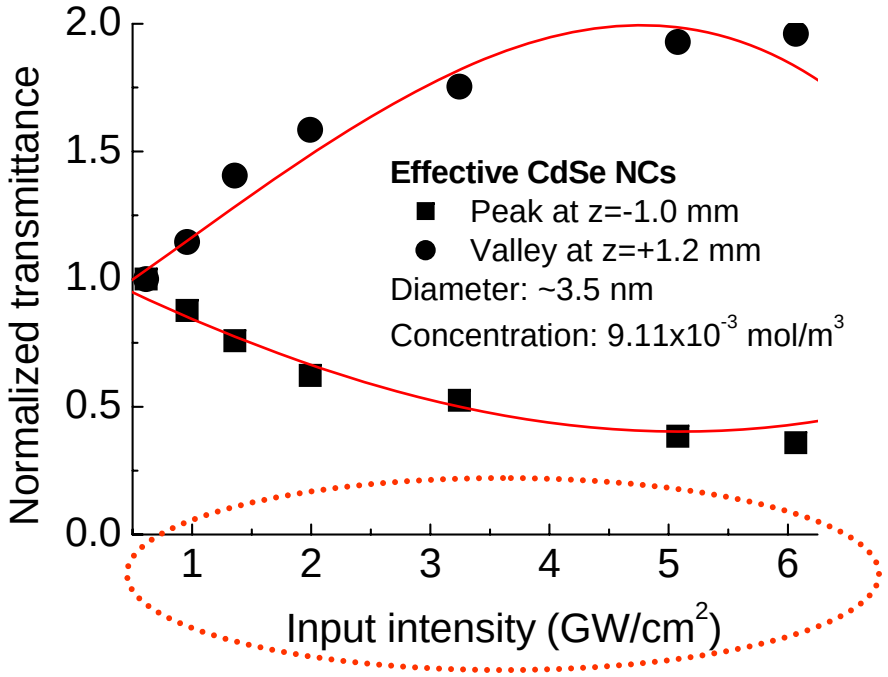

- Resonant Excitation with 8-ns pulse width at ~532 nm
  - Limiting threshold: ~3.2 GW/cm^2

- Requirement to improve the power limiting effect

Conclusion

- CdSe Quantum Dots
  - Size: ~3.5 nm
  - Nonlinear refraction:
    - γ : ~ -9.55×10^{-18} m^2/W (resonant excitation)
    - Negative nonlinearity (self defocusing) properties
  - Nonlinear absorption:
    - β: ~ 4.49×10^{-11} m/W (resonant excitation)
    - Two-step absorption
  - Hyperpolarizability:
    - Parallel DFWM:
      - $\langle\gamma^h_{xxxx}\rangle$ ~1.59x10^{-26} esu (resonant excitation), $\langle\gamma^h_{xxxx}\rangle$ ~1.02x10^{-28} esu (nonresonant excitation)
    - Orthogonal DFWM
      - $\langle\gamma^h_{xyyx}\rangle$ ~5.43x10^{-27} esu (resonant excitation), $\langle\gamma^h_{xyyx}\rangle$ ~3.41x10^{-29} esu (nonresonant excitation)
    - Ratio $\langle\gamma^h_{xyyx}\rangle$ / $\langle\gamma^h_{xxxx}\rangle$ ~0.34 (both the resonant and nonresonant excitation)
      - A large contribution of electronic polarization process to the third-order nonlinearity of CdSe Q-dots

- Nonlinear transmittance effects:
  - Concentration: ~9.11 x10^{-3} mol/m^3
  - Tansmittance threshold of CdSe Q-dots: ~ 3.2 GW/cm^2 (resonant excitation)